Study of the interaction between major compounds of the essential oils of Java citronella and cinnamon and the plasma plant membrane

Auteur : Foncoux, Bérénice
Promoteur(s) : Lins, Laurence
Faculté : Gembloux Agro-Bio Tech (GxABT)
Diplôme : Master en bioingénieur : chimie et bioindustries, à finalité spécialisée
Année académique : 2018-2019
URI/URL : http://hdl.handle.net/2268.2/8036

Study of the interaction between major compounds of the essential oils of Java citronella and cinnamon and the plasma plant membrane

Bérénice Foncoux

Master Thesis presented for the obtention of the bioengineer master diploma option chemistry and bio-industry

Academic year 2018-2019

Promoter: Dr Laurence Lins

Study of the interaction between the major compounds of the essential oils of Java citronella and cinnamon and the plasma plant membrane

Bérénice Foncoux

Master Thesis presented for the obtention of the bioengineer master diploma option chemistry and bio-industry

Academic year 2018-2019

Promoter: Dr Laurence Lins

Laboratory

This thesis was realized at the Laboratory of Molecular Biophysics at the Interface at Gembloux Agro-bio Tech (Liege University).

Remerciements

Tellement de personnes à remercier et jamais les bons mots pour le dire.

Je tiens tout d'abord à remercier Laurence Lins pour son aide précieuse, sa gentillesse et sa patience. Merci Laurence pour l'opportunité que vous m'avez offerte et pour m'avoir si bien accompagné dans de mon TFE.

Je remercie également toute l'équipe du Laboratoire de Biophysique Moléculaires aux Interfaces. Merci à Magali Deleu pour m'avoir aidée et conseillée, à Catherine Chemotti pour son aide, sa patience et sa gentillesse et à Estelle Deboever pour ses explications et sa bonne humeur contagieuse.

Je voudrais remercier spécialement Yoann Laurin pour m'avoir encadrée durant ma thèse et Gaëlle Redouté avec qui j'ai le plaisir de faire mon TFE, pour leurs explications, leurs encouragements, pour leur optimisme inébranlable et pour tous ces moments qui ont fait de mon TFE une expérience si riche.

Je remercie tout particulièrement ma famille qui m'a encouragée, soutenue et rassurée. Merci pour votre amour inconditionnel qui m'a porté toutes ces années.

Je tiens aussi à remercier tous mes amis qui ont fait de ces cinq années les plus belles et particulièrement aux chimistes qui les ont rendus fantastiques. En particulier, un tout grand merci à Aurélie, Guillaume, Gwendoline, Olivier et la bande qui m'ont accompagné de leur folie et qui ont réussi à me supporter pendant si longtemps.

Enfin, merci à mon kot, le kot BV pour toutes ces expériences qui m'ont littéralement marqué à jamais.

Bref, merci à tous pour ces magnifiques années et amitiés inoubliables au sein de ces vieux murs de Gembloux et merci à vous qui lisez ce TFE.

Abstract

Since the 50s, the massive and “environmental naïve” use of synthetic chemistry has revolutionized the farming community facing the dramatic growth of demography. However, nowadays the controversy grows about the long-term harmful effects of these products on human health and the environment. In this context, the use of essential oils (EOs) could be an alternative to chemical products. To develop EOs as bioherbicides, a better understanding of their mode of biological action for new and optimal applications is of importance. Indeed, if the biocidal effects of some EOs or their components have been at least partly elucidated at the molecular level, very little is currently known about their mechanism of action as herbicides at the molecular level.

In a previous study, the cinnamon and Java citronella essential oils and their main components, cinnamaldehyde (CIN), citronellal (CitA) and citronellol (CitO) were shown to be efficient herbicides. The individual EO molecules are small amphiphiles allowing them to cross the mesh of cell wall and interact directly with the plant plasma membrane (PPM), one of the potential cellular targets of EOs.

We used here an integrative biophysical approach combining Molecular Dynamics, Isothermal Titration Calorimetry and Langmuir trough to investigate and characterise the interaction between CIN, CitA and CitO and biomimetic PPM. We showed that if CitO and CitA having a similar chemical structure, are able to interact with the model membranes without permeabilizing effect, CIN belonging to the phenylpropanoid family, is not. We suggested that different mechanisms of action for the two types of molecules can occur: while the monoterpenes could disturb the lipid organization and/or domain formation, the phenylpropanoid CIN could interact with membrane receptors.

Résumé

Depuis les années 50, l'utilisation massive et "naïve" de la chimie de synthèse a révolutionné le monde agricole face à la forte croissance démographique. Cependant, la controverse grandit sur les effets nocifs à long terme de ces produits sur la santé humaine et sur l'environnement. Dans ce contexte, l'utilisation des huiles essentielles (EO) pourrait être une alternative aux produits chimiques. Pour cela, une meilleure compréhension de leur mode d'action biologique pour des applications nouvelles et optimales est importante. En effet, si les effets biocides de certaines EO ou de leurs composants ont été au moins partiellement élucidés, on en sait actuellement très peu sur leur mécanisme d'action en tant qu'herbicides au niveau moléculaire.

Dans une étude précédente, les huiles essentielles de cannelle et de citronnelle et leurs principaux composants, le cinnamaldéhyde (CIN), le citronellal (CitA) et le citronellol (CitO) se sont révélés efficaces comme herbicides. Les molécules d'EO sont de petits amphiphiles qui peuvent traverser le maillage de la paroi cellulaire et interagir directement avec la membrane plasmique végétale (PPM), l'une des cibles cellulaires potentielles des EO.

Nous avons utilisé ici une approche biophysique intégrative combinant la dynamique moléculaire, la calorimétrie par titrage isotherme et la cuve de Langmuir pour étudier et caractériser l'interaction entre CIN, CitA et CitO et la PPM biomimétique. Nous avons montré que si CitO et CitA ayant une structure chimique similaire, sont capables d'interagir avec les membranes du modèle sans effet de perméabilisation, CIN appartenant à la famille des phénylpropanoïdes, en est incapable. Nous avons suggéré différents mécanismes d'action possible pour les deux types de molécules : alors que les monoterpènes pourraient perturber l'organisation lipidique et/ou la formation de domaines, les CIN phénylpropanoïdes pourraient interagir avec des récepteurs membranaires.

List of abbreviation

Abbreviations	Meaning
EO	Essential oil
PPM	Plasma Plant Membrane
CitO	Citronellol
CitA	Citronellal
CIN	Cinnamaldehyde
PM	Plasma membrane
S_O	Solid-ordered phase
L_D	Liquid-disordered phase
L_O	Liquid-ordered phase
GIPC	Glycosyl inositol phosphorylceramides
GluCer	Glucosylceramides
PLPC	Palmitoyl linoleoyl phosphatidylcholine
SUV	Small Unilamellar Vesicles
LUV	Large Unilamellar Vesicles
GUV	Giant Unilamellar Vesicles
ITC	Isothermal Titration Calorimetry
FTIR	Infrared spectrometry
MD	Molecular dynamics
PBC	Periodic Boundary Conditions
RMSD	Root Mean Square Deviation
MLV	Multilamellar Lipid Vesicles
MIP	Maximal Insertion Pressure
dΠ0	Differential Π0

List of figures

List of tables

Table of content

INTRODUCTION

A. Context

After the second world war, the rapid demographic growth led to the necessity for greater crop yield. To lessen the losses caused by pests and weed population in agricultural field, massive and abusive use of pesticides was made. In the 90s, the realisation of the detrimental impact of pesticide abuse led to a new trend toward agricultural sustainability where only the needed quantity was applied to a field. However, the simple use of chemical pesticides is now being put into question. The long-lasting environmental damages, the possible health risks and the development of weed resistance highlight the need for a more environmentally friendly weed management.

It has been predicted that the world's population will grow to reach 10 billion in 2050 (FAO, 2017). To sustain such a growth in demography, the food production will need to be increased by approximately 70% between 2005 and 2050 (FAO, 2009). With growing needs but finite resource, there is a clear necessity to increase crop yield.

Weed population in agricultural field being one of the major reasons for crops yield reduction (Radhakrishnan, Alqarawi and Abd_Allah, 2018), weed management is a key to the reduction of agricultural losses and remains a challenge (Tworkoski, 2006). Strategy for weed management varies but modern agriculture mostly relies on synthetic herbicides because of their efficiency in preventing the germination and growth of weeds.

As said above, herbicides are nowadays under controversy. First, herbicides are often used in unsuited amount (Green, 2014; Osteen and Fernandez-Cornejo, 2016). Moreover, synthetic herbicides most often contain one or two active components (Mortimer, 1997), are used without rotation programmes and target the same site of action at the molecular level (Beckie *et al.*, 2011). This has caused a rise in the development of resistant germplasms (Mortimer, 1997; Owen, 2016). Furthermore, those herbicides can impact the environment and human health due to their toxicity, persistence in the environment and bioaccumulation in organisms (Searchinger *et al.*, 2013; Zhang, 2018). These drawbacks have led to the search for alternatives, notably natural molecules more respectful of the environment and with new mechanisms of action.

A promising alternative is bioherbicides. Bioherbicides are products synthesised by living organisms or their natural metabolites to control weed population (Radhakrishnan, Alqarawi and Abd_Allah, 2018). Their novel and plural mechanisms of action and their relatively quick degradation in the environment makes them good candidates to replace synthetic herbicides.

To assess their potential as herbicides, studies must first be conducted on their exact mechanisms and sites of action. This master thesis studies the molecular effects of the main components of the essential oils of cinnamon and Java citronella on the plasma plant membrane (PPM), one of the possible targets of these bioherbicidal molecules, to enable further studies of the rational use of essential oils as bioherbicides.

STATE OF THE ART

A. Essential oils

a. Generalities

Essential oils are defined as hydrophobic oils composed of volatile aromatic compounds naturally present in plants. The compounds composing EO, also known as secondary plant metabolites, give to plants their distinctive scent and flavour. They can be found as droplets in the flowers, seeds, bark, wood, roots, leaves and fruits of aromatic plants. EO are produced in plant organs such as secretion ducts, epidermal cells or glandular trichomes by intracellular biogenetic pathways. An EO is composed of 20 to 70 different secondary metabolites with one to five predominant compounds which usually determine the properties of the oil (Pavela, 2015). The composition, quality and quantity of an EO can vary with environmental, genetic, and climatic factors, nutritional status of the plants, and other factors.

EOs have been used since the Middle Age for their fragrance, their antibacterial, antiviral, antifungal, insecticidal and medicinal properties. With the renewed interest of the public for natural products, EOs are once again under scrutiny. Nowadays, essential oils are used in cosmetics, foods and in the agriculture industry (Burt, 2004). Their effects as antimicrobials are actually the most studied in the literature.

The EOs' components can be divided in two main classes: the first one comprising terpenes and terpenoids while the second one includes aromatic and aliphatic constituents. These two classes of constituents are formed by different precursors and pathways. The secondary metabolites forming the EOs can be of various chemical classes such as alcohols, ethers or oxides, aldehydes, ketones, esters, amines, amides, phenols and heterocycles. Figure 1 shows different types of essential oils' components and their chemical function.

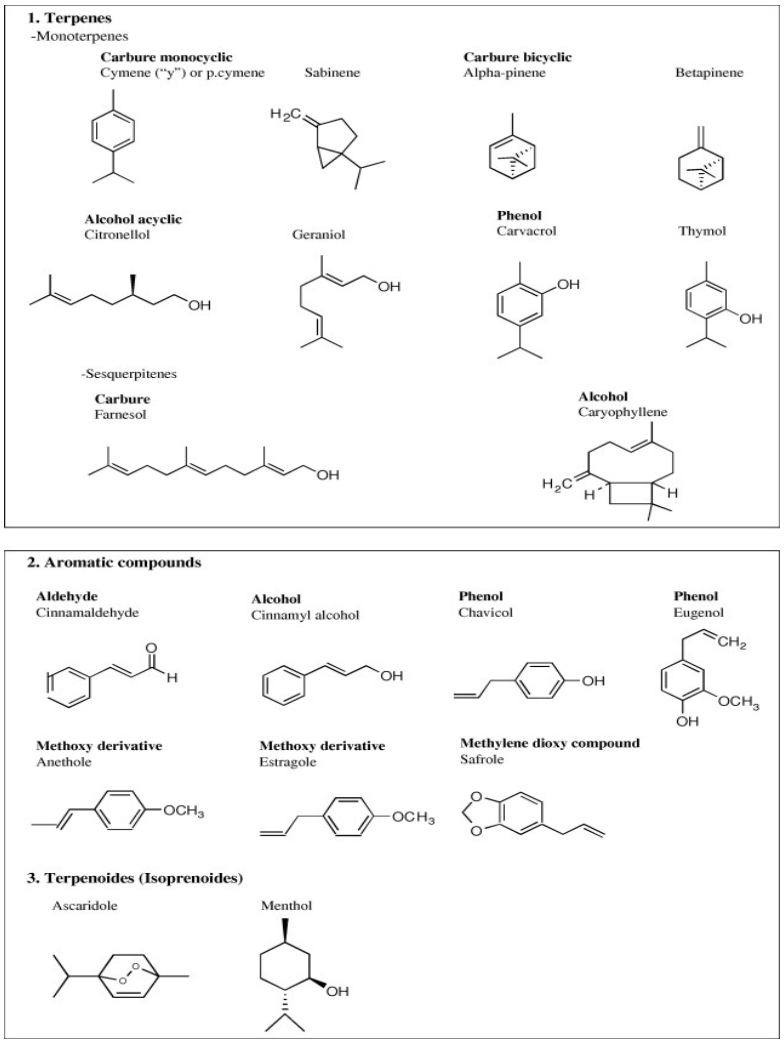

Figure 1: Structure of some essential oil components and their chemical function (Bakkali et al., 2008).

Terpenes are a large class of hydrocarbon compounds constructed from five-carbon isoprene units (C_5H_7) that are assembled to form the backbone of the molecule on which chemical groups can be added (Tidgewell, Clark and Gerwick, 2010). The isoprene units, also called 2-methyl-1,3-butadien, are condensed following a head-to-tail model. Figure 2 shows the structure of isoprene on which EO components are based. The diverse possible conformations for isoprene allow for various chemical features and properties.

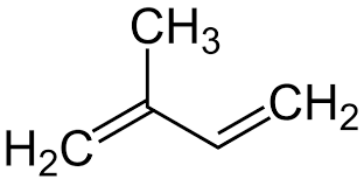

Figure 2: Structure of isoprene.

The terpenes found in EOs are mainly made of mono- and sesquiterpenes. Monoterpenes are constructed from two isoprene units via the methyl-erithrytol pathway and constitute 90% of the essential oils, while sesquiterpenes are made of three units of isoprene via the

mevalonate pathway (Dilworth, Riley and Stennett, 2017; Nazzaro *et al.*, 2017). Terpenoids are enzymatically derived from terpenes but they contain additional oxygen molecules or a rearrangement of methyl groups. They are also produced by the mevalonate pathways.

The second class of essential oils are aromatic and aliphatic constituents such as cinnamaldehyde, eugenol, and safrole. Aliphatic compounds are made up of carbon chains and don't have a ring while aromatic molecules contain a benzene ring and can comprise a polycyclic structure. The most common aromatic and aliphatic compounds are esters and aldehydes (Sterrett, 1962). They are made via the shikimic acid pathway (Dilworth, Riley and Stennett, 2017) but occur less frequently than terpenes (Eslahi, Fahimi and Sardarian, 2017). Figure 3 shows the aromatic, mono- and sesquiterpenes structures of several EO components.

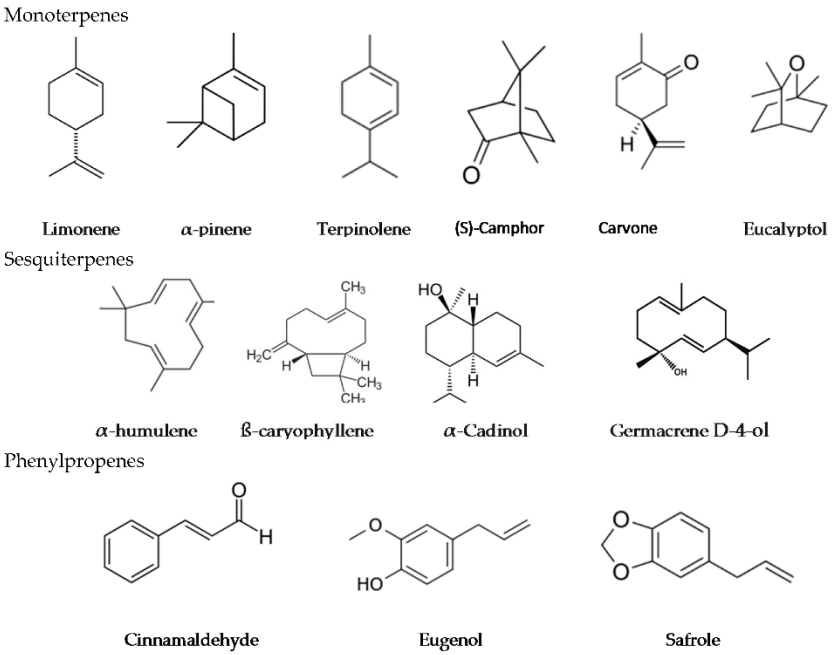

Figure 3: Structure of some terpenic and aromatic essential oil components (Gnankiné and Bassolé, 2017).

b. Essential oils' effects

It has been shown that essential oils have a detrimental effect on Gram-positive and Gram-negative bacteria (Reichling *et al.*, 2009; Mnif *et al.*, 2016; Semeniuc, Pop and Rotar, 2017). Considering the wide diversity of essential oils and their components, it is highly likely for different components to have different molecular mechanisms and targets (Cavalieri and Caporali, 2010). Nonetheless, several EOs seem to alter the membrane fluidity and permeability (Tworkoski, 2006; Bouyahya *et al.*, 2019), as shown by the leakage of ions and other cell contents, the inhibition of cell respiration and the depletion of intracellular ATP (Laosinwattana, Wichittrakarn and Teerarak, 2018; Hu *et al.*, 2019; Kang *et al.*, 2019).

Eukaryotic cells notably fungi, insects and plants, are also affected by essential oils. Hammer *et al.* (2004) showed that the tea tree oil increases the membrane permeability and fluidity of *Candida albicans* and *Candida glabrata* which in turn causes electrolytes leakage and cellular

death. According to Pinto *et al.* (2006), the essential oil of thyme causes lesion to the cytoplasmic membrane and reduces the ergosterol content of the lipid bilayer of Candida, Aspergillus and dermatophyte species. Nazzaro et al. (2017) also point out that EOs can cause distortion and damage to the cell wall and the cell membrane of Candida species. They can also induce modifications of the cell morphology and alter the Reactive Oxygen Species (ROS) production.

Essential oils cause insects' death by impairing the anti-oxidant defence system (Kiran *et al.*, 2017), decreasing the integrity of the DNA (Castillo-Morales *et al.*, 2019) and impairing the mitochondrial respiration and membrane. It also affects the neuronal activity through acetylcholinesterase (AChE) inhibition (Castillo-Morales *et al.*, 2019; Rajkumar *et al.*, 2019), through the interference of the GABA-gated chloride channels and through the targeting of the neurotransmitter, neuromodulator and neurohormone Octopamine (Pavela, 2015).

The herbicidal effect and the reduction of seed germination and plant growth caused by essential oils has been demonstrated in numerous publications. Cellular death could be caused in part by the leakage of electrolytes and other cellular constituents which denotes a loss of membrane integrity (Tworkoski, 2006; Singh *et al.*, 2009; Poonpaiboonpipat *et al.*, 2013; Laosinwattana, Wichittrakarn and Teerarak, 2018). Another possible mechanism for cellular death is the induction of oxidative stress shown by the overproduction of ROS (Singh *et al.*, 2009; De Martino *et al.*, 2010; Khare *et al.*, 2019). ROS are naturally produced by the cell but in excessive quantity, it can lead to membrane disruption, enhanced lipid peroxidation and impairment of the photosynthetic activity. The malfunction of the photosynthetic machinery is demonstrated by the reduction of chlorophyll and carotenoids content (Poonpaiboonpipat *et al.*, 2013; Laosinwattana, Wichittrakarn and Teerarak, 2018).

The reduction of seed germination is concomitant to the decrease of the induction of α-amylase (Poonpaiboonpipat *et al.*, 2013; Laosinwattana, Wichittrakarn and Teerarak, 2018). Alpha-amylase is a protein that degrades the reserve carbohydrates into soluble sugars which is a necessary step of germination.

Singh *et al.* (2009) reported that plant growth could be inhibited by killing of meristematic cells, suppression of mitotic activity and membrane disintegration.

By comparing the effect of essential oils on bacteria, fungi, insects and plants, we can note that the exact mechanisms of action and the molecular targets are often unknown and can differ, but there are also similarities in how they affect the cells. In particular, the membrane seems to play a major role in the interaction between essential oils and prokaryotic or eukaryotic cells. Thus, it can be hypothesized that the plasma membrane is a molecular target of EOs. One of their possible mechanisms of action could be through the disruption of the membrane or its modification. EOs might insert into the fatty acyl chains that form the lipid bilayer causing changes to membrane properties. Indeed, EOs' hydrophobic properties enable them to interact with the hydrophobic part of the membrane.

B. Essential oils of Java citronella and cinnamon

A previous master thesis carried out in the host lab has studied the composition and the quantification of the essential oils of *Cinnamomum zeylanicum* Blume (cinnamon) and *Cymbopogon winterianus* Jowitt (Java citronella) (Dal Maso, Lins and Fauconnier, 2016). Their effects on *Arabidopsis thaliana* (L.) Heynh was further investigated.

The cinnamon EO was found to contain 60 different compounds while the Java citronella EO was composed of 57 molecules. The main components of the cinnamon EO is cinnamaldehyde (71.80%) followed by eugenol, caryophyllene, cinnamyle acetate and linalool respectively. The composition of the Java citronella EO was citronellal (37.59%), geraniol (21.94%), citronellol (14.06%) and limonene (5.63%). The other compounds were present in lesser amount. The damages of the whole EOs and their main components on the leaves and cotyledons of *A. thaliana* can be seen in Figure 4.

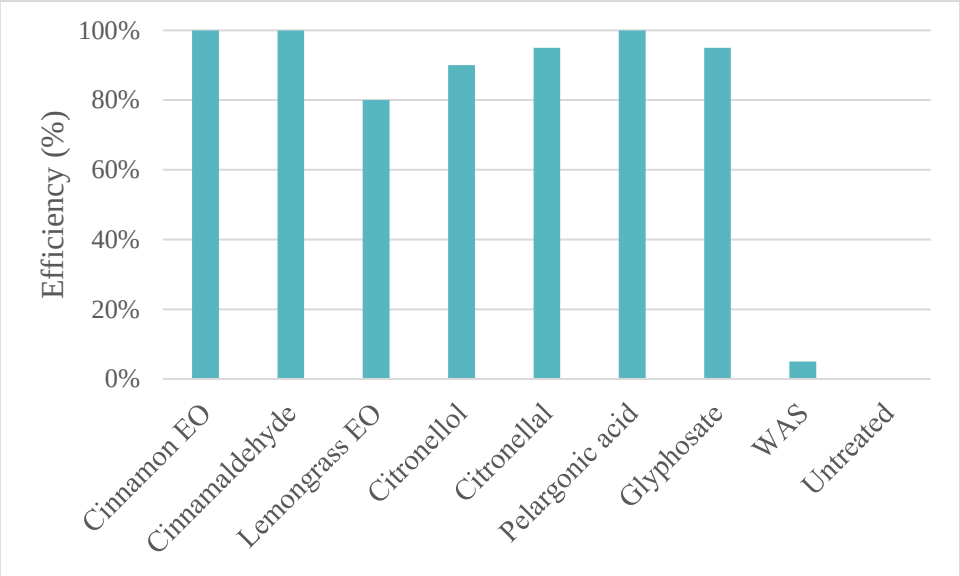

Figure 4: Damages observed on A. thaliana leaves (in %) after a treatment with cinnamon and Java citronella EOs and their main components, cinnamaldehyde, citronellol and citronellal at 3% compared to pelargonic acid (0.72%) and glyphosate (3%). Untreated plants and plants treated without active substances (WAS) (1% Tween and 0.5% ethanol) were used as reference – n=5.

The herbicidal effect of Java citronella EO was already described by Poonpaiboonpipat *et al.* (2013) and that of cinnamon EO by Tworkoski (2006), Cavalieri and Caporali (2010), and Radhakrishnan, Alqarawi and Abd_Allah (2018) respectively. However, because of the high variability between essential oils even of the same species, it is more relevant to analyse the effects of the EO components, namely cinnamaldehyde for cinnamon and citronellal and citronellol for Java citronella. The three components are as active as the complete EOs and as commercial herbicides (Fig. 4).

a. Citronellol

Citronellol (CitO), also called 3,7-Dimethyloct-6-en-1-ol, is an alkene substituted by a hydroxy group at position 1 and methyl groups at positions 3 and 7. Its hydrocarbon structure makes the molecule lipophilic with an octanol/water partition coefficient of 3.91. However, its hydroxy group enables the formation of hydrogen bonds with hydrophilic molecules. In nature, both the (+)- and (-)-citronellol exist. The structure of (+)-citronellol is shown in Figure 5.

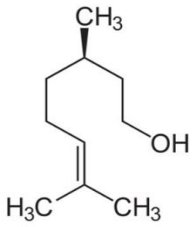

Figure 5: Structure of (+)-citronellol.

The enantiomer present in *Cymbopogon winterianus* Jowitt and used in this study is the (+)-citronellol which is more potent than its (-) counterpart (Tidgewell, Clark and Gerwick, 2010).

CitO has antibacterial, antifungal, lipolytic, anti-allergic, anti-inflammatory, cardiovascular and antidiabetic effects (Matos *et al.*, 2018). The insecticidal properties of CitO and its effect against egg rafts, larvae and adult insects was demonstrated by Tabari *et al.* (2017). CitO is also able to reduce the germination and radicle length of radish and garden cress seeds (De Martino *et al.*, 2010).

Several sources linked the antifungal effect of CitO with its effects on the cell membrane. Tao, Jia and Zhou (2014) showed that the application of CitO on *Penicillium italicum* and *Penicillium digitatum* leads to the disruption of the cell membrane followed by the leakage of cell constituents. These results are in agreement with the publication of De Oliveira Pereira *et al.* (2015) that suggested that cell disruption is linked to a modification of ergosterol production caused by CitO. This hypothesis was supported by Sharma *et al.* (2019) who indicated that it has a depleting effect on the ergosterol membrane content. Lim and Shin (2009) demonstrated that CitO's effects on the membrane are not only due to the impairment of ergosterol biosynthesis but also to a change in the lipid composition or biosynthesis of the cell membrane.

The herbicidal effects of CitO on root and shoot growth of *Triticum aestivum* was studied by Kaur *et al.* (2011). They highlighted how CitO enhances solute leakage and induces the ROS generation. They put forward the hypothesis that ROS production results in lipid peroxidation and membrane damage.

b. Citronellal

Citronellal, also called 3,7-Dimethyloct-6-enal, is a monoterpenoid and an aldehyde that can be found in the plant of genus *Cymbopogon.* Citronellal (CitA) is the main component of the essential oil Java citronella and gives it its typical lemon scent. It is a hydrophobic molecule with an octanol/water partition coefficient of 3.53. The aldehyde chemical function also allows the formation of hydrogen bonds. In nature, both the (+)- and (-)-citronellal exist. The enantiomer predominantly present in *Cymbopogon winterianus* Jowitt and used in this study is the (+)-citronellal (Cahyono *et al.*, 2014) (Fig. 6).

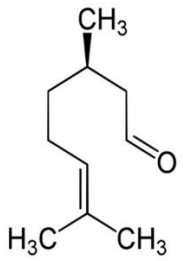

Figure 6: Structure of (+)-citronellal.

Several publications related that CitA has fungicidal, insecticidal and herbicidal activities. It was also shown that it has an antinociceptive effect in mice where it induces ataxia, analgesia and sedation (Melo *et al.*, 2010). CitA also presents anti-inflammatory and redox protective properties in mice (Melo *et al.*, 2011).

In *Candida albicans*, CitA was shown to modify the membrane fluidity and interfere with membrane bound signalling proteins (Zore *et al.* (2011)). It was also found to damage the cell membrane, to reduce ergosterol levels by 50% and to lessen the plasma membrane ATPase activity by diminishing the glucose-induced H^+ extrusion (Singh, Fatima and Hameed, 2016). CitA also inhibits the mycelial growth and spore germination of *Penicillium digitatum* by deteriorating the plasma membrane of the fungus' spores, leading to a higher extracellular conductivity and release of cell constituents (Nazzaro *et al.*, 2017).

As insecticide, CitA causes a mortality of 78% in the pest *Ascia monuste*'s larvae (Ribeiro *et al.*, 2018) and it decreases egg hatching, larvae development and insect mobility of the nematode parasite *Haemonchus contortus* (Araújo-filho *et al.*, 2018).

As herbicide, CitA was found to decrease the germination of *Digitaria horizontalis* and *Cenchrus echinatus* by 98% and to diminish the chlorophyll and total protein content in cell by 80% and 90% respectively (Cangussu *et al.*, 2017). CitA was also shown to inhibit weed emergence and early seedling growth both in the roots and the shoots. The reduced growth was more pronounced in the roots than the shoots and was due to the suppression of the mitotic activity of growing root tip cells. The application of CitA also leads to chlorosis and necrosis of the plant *Cassia occidentalis* caused by a loss of chlorophyll and the reduction of cell respiration (Singh *et al.*, 2002, 2006). After analysing the leaves, it was found that CitA triggered disruption of cuticular wax, clogging of stomata and rapid electrolyte leakage. The

rapid electrolyte leakage was shown to be the consequence of the disruption of the membrane integrity in different weed species (Singh *et al.*, 2004, 2006).

c. Cinnamaldehyde

Cinnamaldehyde (CIN) is a phenylpropanoid synthesized in the bark of the genus species *Cinnamomum* and gives its odour and flavour to cinnamon. CIN, or (2*E*)-3-Phenylprop-2-enal, is formed of an aromatic cycle and an aldehyde which gives it the capacity to interact with both lipophilic and hydrophilic molecules. Its water/octanol partition coefficient is 1.90. It is predominantly found in its trans (E) form (Fig. 7).

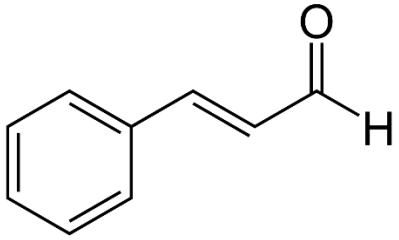

Figure 7: Structure of trans-cinnamaldehyde.

CIN's effects were mostly observed on bacteria, fungi and insects. It is also shown to have an antioxidant and anti-inflammatory activity in rheumatoid arthritis patients (Mateen *et al.*, 2019) and antidiabetic effect in rats (Subash Babu, Prabuseenivasan and Ignacimuthu, 2007). To our best knowledge, only one publication studied the herbicidal effect of CIN.

The antibacterial effects of CIN on several bacteria were studied by Kalemba and Kunicka (2003). They notably reported that the minimal inhibitory concentration was 31µg/ml for *Haemophilus influenzae* and 250µg/ml for *K. pneumoniae*. Shreaz *et al.* (2016) reviewed the antifungal properties of CIN. The application of CIN leads to a decrease in the germination of *A. flavus*' spores and a change of the morphology and ultrastructure of its hyphae and spores (Shreaz *et al.*, 2016). CIN was shown to be toxic against *Tribolium castaneum*'s and *Sitophilus zeamais*'s larvae and insects (Huang and Ho, 1998).

The impact on CIN on the plasma membrane can differ. Mnif *et al.* (2016) reported that it can inhibit the growth of *Escherichia coli* and *Salmonella typhimirium* without disintegrating the membrane or depleting intracellular ATP. However, it was also found that CIN's application on *Escherichia coli* and *Staphylococcus aureus* leads to a separation of the membrane from the cell wall and to cell membrane lysis, cytoplasmic content condensation and leakage, cytoplasmic content depolarization and cell distortion (Shen *et al.*, 2015). CIN was shown to interact with the membrane of *Candida albicans* by reducing its ergosterol content by 55% (Shreaz *et al.*, 2010). It also increases the ROS production and impairs the cell membrane permeability and the cell wall integrity of *Penicillium italicum* (Huang *et al.*, 2019).

CIN was showed an inhibitory effect on seed germination, shoot and root growth of Chinese amaranth (*Amaranthus tricolor* L.) by 54.55%, 75.53%, and 85.13% respectively (Chotsaeng,

Laosinwattana and Charoenying, 2018). It could also reduce seedling shoot growth of barnyard grass (*Echinochloa crus-galli* (L.) Beauv) by 27.83% and root growth by 46.20%.

C. Plasma membrane

a. Generalities

The plasma membrane (PM) is the structure delimiting the cell and it functions as the point of exchange with the external environment and bordering cells. Its role as a selective barrier is to take up water and essential minerals, to realise gas exchange, to perceive and transport signalling molecules and to discern modifications of the cellular environment. The plasma membrane is primarily composed of a lipid bilayer embedded with proteins. A schematic structure of the asymmetrical membrane is given in Figure 8.

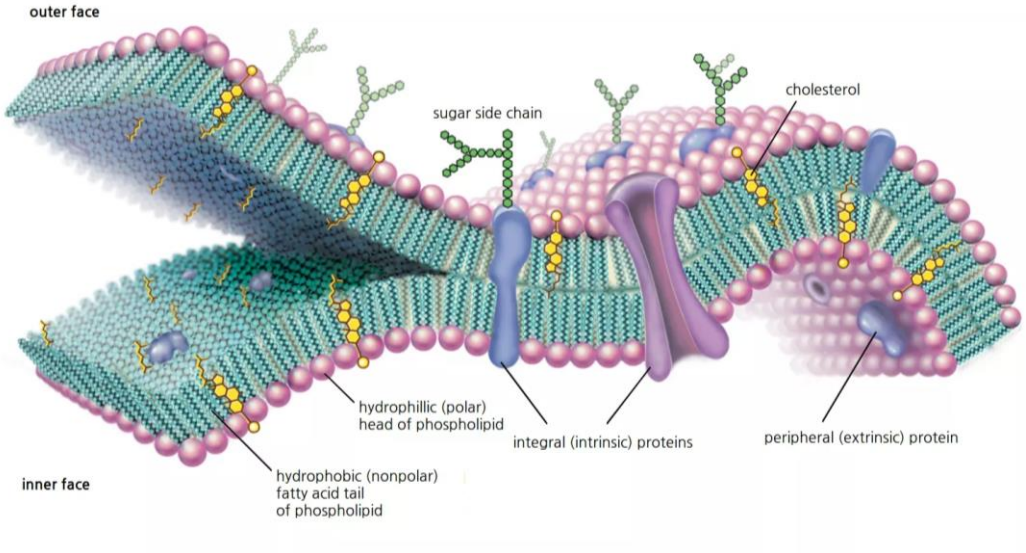

Figure 8: Schematic structure of the Plasma membrane (*Encyclopædia Britannica,* Inc.).

As shown in Figure 8, the proteins can be peripheral or crossing the membrane. The peripheral proteins are linked to the membrane by electrostatic force or hydrogen bonds while integral proteins are intimately inserted into the hydrophobic core of the bilayer. They notably play a role in structuring the membrane, transporting molecules across the membrane or transmitting signals to the cytoplasm. Proteins were long thought to be the main actors of the cell physiological functions but the lipids composing the bilayer also play fundamental roles. Lipids are notably important to determine cell structures, regulate membrane fluidity and transduce signals.

The composition and physical state of the lipid bilayer influence lipid–protein and protein–protein associations, membrane-bound enzyme activities, and transport capacity of membranes. The PM shouldn't be considered composed of independent molecules but should be considered

as an interdependent lipid-protein composite. For instance, a very high density of membrane proteins may modify the order of neighbouring lipids and cause changes in the gating of a protein channel (Moe and Blount, 2005).

b. Lipid classes

The PM is composed of three main classes of lipids: sterols, sphingolipids and glycerolipids. Their structures and chemical features can be seen in Figure 9.

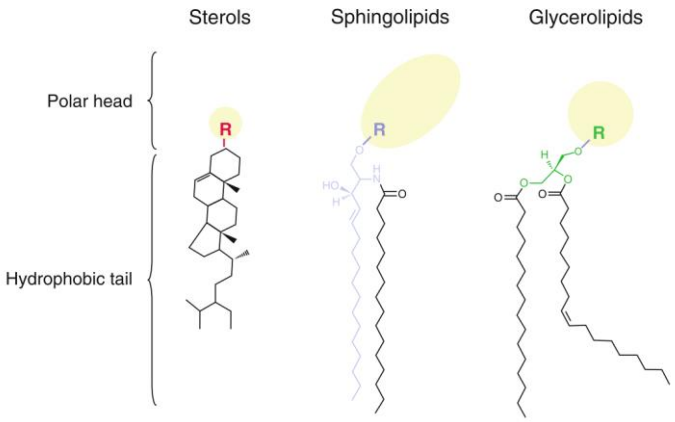

Figure 9: Structures of the three major classes of plant plasma membrane and their chemical features (Furt, Simon-Plas and Mongrand, 2010).

Glycerolipids are tripartite molecules made of a glycerol moiety linked to at least one fatty acyl chain. Glycerophospholipids, the principal subclass of structural lipids in eukaryotic membranes, are composed of two fatty acyl chains esterified to a glycerol moiety which is also linked to a phosphate group. The phosphate group can be further esterified with choline, ethanolamine, serine or inositol (Casares, Escribá and Rosselló, 2019). They are amphipathic lipids abundant in the lipidic bilayer that can interact with other lipids and proteins. Glycerophospholipids are present in the membrane as a wide variety of species that differ by their headgroup and fatty acyl chains composition. In mammalian membranes, the fatty acyl chains are predominantly stearic acid (18:0) and oleic acid (18:1), whereas plant plasma membranes are enriched in palmitic (16:0), linoleic (18:2), and linolenic (18:3) acids (Wayne, 2019). Glycerophospholipids are mostly known for their structural role in the membrane, but they are also involved in various key biological and physiological activities and in the transduction of extracellular signals.

Sterols are a subgroup of steroids present in the membrane of plants, fungi and animals. The only sterol presents in animals and fungi is cholesterol and ergosterol respectively while plant sterols are varied (see point d.). Sterols are isoprenoids made of a sterane backbone composed of four rings which confers to sterols a high rigidity. The sterane backbone (Fig. 10) is connected to a hydroxyl group, that acts as the headgroup of the lipid. Sterols regulate biological processes and are important for membrane fluidity and regulating the physico-chemical the

properties of the membrane. Indeed, sterols increase the order of fluid phases even when the acyl part of their hydrophobic tail contains unsaturations (Dufourc, 2008).

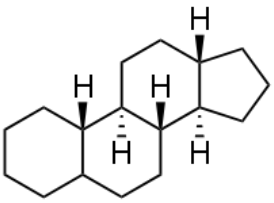

Figure 10: Structure of sterane.

Sphingolipids are composed of a backbone of sphingoid bases, also called Long Chain Bases (LCB) upon which functional groups are added. One of the simplest examples of sphingoid base is the sphingosine molecule (Fig. 11) which is constituted of at least two hydroxyl functions, a fatty acid chain and an amine function. LCB represents the first class of sphingolipids while the second class of sphingolipids is the ceramides. The latter are formed by the addition of a fatty acyl chain to the amine function. Sphingolipids are bioactive signalling molecules that play a structural role, regulate signal transduction pathways and mediate cell-to-cell interactions and recognition (Bartke and Hannun, 2009). It has been shown that sphingolipids' physicochemical features allow them to interact with other membrane constituents and cluster with sterols (Masserini and Ravasi, 2001). The microdomains formed by sterols and sphingolipids are important for the PM properties and function.

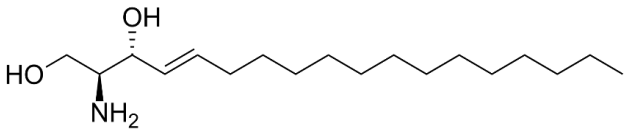

Figure 11: Structure of sphingosine.

c. Importance of the lipid composition

PM can occur in different physical states. The two commonly known states are the solid-ordered phase and the liquid-disordered phase, also called the liquid crystalline phase. The solid-ordered phase or S_0 is a more organized state, a solid-like state, where the lipids have little mobility. The liquid-disordered phase or L_D is a more disorganized, liquid-like state where lipids have a higher mobility. The change from one state to the other is called the transition phase and is characterized by a phase transition temperature.

Each lipidic species, influenced by its chemical structure, has a phase transition temperature. The nature of the headgroup, the length of the hydrophobic tail, the number and position of unsaturations in the fatty acyl chain all impact the compactness of a lipid. Indeed, a greater chain length leads to an increased interaction between hydrocarbons and compactness. On the contrary, double bonds cause a twist in the chain, reducing the interaction (Wayne, 2019). The higher the proportion of ordered lipids in the PM, the more stable and compact the membrane will be and the higher the phase transition temperature will be.

There exists a third state of the PM, a more ordered intermediate phase between the S_O and the L_D phase called the Liquid-ordered phase (L_O phase) (Brown and London, 2002). This L_O phase has both a high rotational or translational mobility and a high conformational order in the lipid acyl chain. It is characterised by a thigh lipid packing. This L_O phase is reached when several unsaturated lipid species interact and create subdomains in the PM. This is notably the case of sterols and sphingolipids (Mongrand *et al.*, 2010; Gronnier *et al.*, 2018). Thus, the insertion of some lipid species in the membrane can lead to the regulation of the lipid chain order and can induce L_O phases (Furt, Simon-Plas and Mongrand, 2010).

d. Lipid composition of the plant plasma membrane

The plant plasma membrane (PPM) is composed of the three classes of lipids cited previously. The predominant class in the PPM is sphingolipids composing 48% of the total PM lipids of tobacco leaves (Cacas *et al.*, 2016). Glycerolipids, mainly present as glycerophospholipids, are the second major class with 30% of the total lipids followed by sterols composing 22% of the PPM lipids of tobacco leaves (Cacas *et al.*, 2016). It is interesting to note that, compared to other cell membranes, the PPM is strongly enriched in sterols and sphingolipids as shown by the sterol-to-phospholipid ratio ranging from 0.6 to 1.5 (Furt, Simon-Plas and Mongrand, 2010).

For glycerophospholipids, phosphatidylethanolamine is the most abundant with 33% followed by phosphatidylcholine with 27% and phosphatidic acid with 20% of total phospholipids of tobacco leaves (Cacas *et al.*, 2016). Phosphatidylglycerol, phosphatidylserine and phosphatidylinositol are also present in the PPM but in lesser amount (Furt, Simon-Plas and Mongrand, 2010). Concerning the fatty acid composition of glycerophospholipids, palmitic (16:0) and linoleic (18:2) chains are the most common with 20 to 60% of the total phospholipids. When they are associated, they compose 35–50% of total phospholipids (Furt, Simon-Plas and Mongrand, 2010).

Contrary to the cell membrane of other organisms which contains one main type of sterol, PPM contains several sterol species which differ by the number and position of double bonds in the cycle, and by the nature of the hydrocarbon chain. Phytosterols can be found as free sterols, steryl glucosides (sterols acylated by a sugar) or acylated steryl glucosides (steryl glucosides further acylated) in the PPM. In most plants and organs, free sterols represent 70 to 90% of total sterols (Furt, Simon-Plas and Mongrand, 2010). However, in tobacco leaves, the proportions of free sterols, acylated steryl glucosides and steryl glucosides are 45%, 36% and 18% of total sterols respectively (Cacas *et al.*, 2016). Sitosterol and stigmasterol are the predominant free sterols present in the PPM (Dufourc, 2008).

PPM can include over 500 different molecular species of sphingolipids. The wide diversity of molecules is due to the presence of various functional groups, the different fatty acyl chains (number and position of unsaturation, length) and the diversity of sphingoid bases. There are eight sphingoid bases composed predominantly of a C18 hydrocarbon chain. The fatty acyl chains of the ceramides are generally composed of 14 to 28 carbons and commonly have an additional molecule linked to the alcohol function. The molecule linked to ceramides can be

one or more sugars which then constitutes glucosylceramides (GluCer) or an inositol monophosphate group which forms the inositol phosphorylceramides. The latter can be further glycosylated to form glycosyl inositol phosphorylceramides also known as GIPC. GIPC are an important class of sphingolipids and unique to plants. Indeed, Cacas *et al.* (2016) have found that GIPC and GluCer represent up to 40% and 8% of total lipids respectively in tobacco plants. However, as GIPC extraction and purification are very difficult, it is not yet well studied.

e. Model membrane

Because of the complexity of the membrane and the diversity of its components, it is very difficult to investigate what happens there at the molecular level. Thus, simplified models are used to study the evolution and interaction of PPM with bioactive molecules. As such, the number of lipid species in the models is limited and controlled, and only the lipid moiety is considered. The lipid composition used in this thesis is chosen to correspond at best to the major lipid components of *Arabidopsis thaliana*.

In *A. thaliana*, the major type of lipids are glycerolipids representing 64% of the total PPM lipids and sterols that constitute 32% of the membrane lipids (Minami *et al.*, 2009). Uemura and Joseph (1995) show that 35.5% of the total lipids are phosphatidylcholine. It appears that 35 to 50% of total phospholipids have a palmitic and a linoleic acid fatty acyl chain (Furt, Simon-Plas and Mongrand, 2010). The major sterols composing the membrane are free sterols such as sitosterol, stigmasterol and campesterol with 85% of total PPM sterols (Minami *et al.*, 2009). Wewer *et al.* (2011) show that sitosterol and campesterol are predominant in *A. thaliana* PM. Another study finds that the most abundant sphingolipids in *A. thaliana* leaves are GIPC with 64% and GluCer with 34% of total sphingolipids (Markham and Jaworski, 2007). However, GIPC being very difficult to extract and purify, it will not be used in this study.

The lipids chosen for this thesis are thus palmitoyl linoleoyl phosphatidylcholine (PLPC), β-sitosterol and glucosylceramide (GluCer) (Fig. 12).

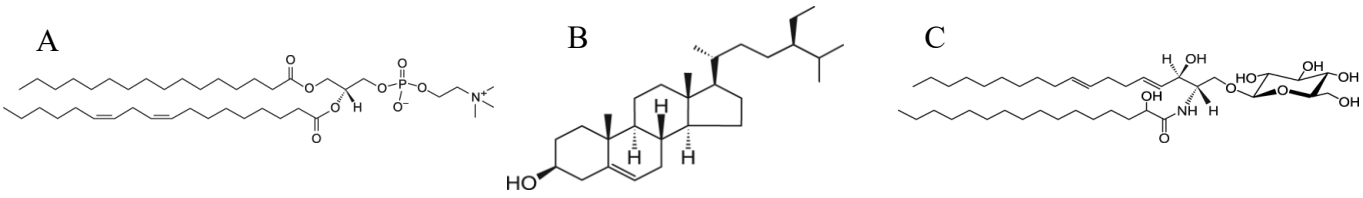

Figure 12: Structure of (A) PLPC, (B) β-sitosterol and (C) GluCer (Avanti Polar Lipids, Inc.).

As model membranes, different types of structures can be used: supported bilayer, lipid monolayer and liposome (Fig. 13). Each structure has advantages and disadvantages and they all mimic to different degrees the biological membrane. The supported bilayer is a flat biomimetic membrane supported onto solid surface. The monolayer represents half the bilayer of a membrane, often the leaflet in interaction with the molecule of interest. Liposomes are spherical vesicles composed of one (unilamellar vesicles) or more bilayers (multilamellar

vesicles). Depending on their size, they are classified into small unilamellar vesicles (SUV), large unilamellar vesicles (LUV) or giant unilamellar vesicles (GUV). Liposomes have the advantage of better representing the biological membrane but are less stable than monolayers or supported bilayers.

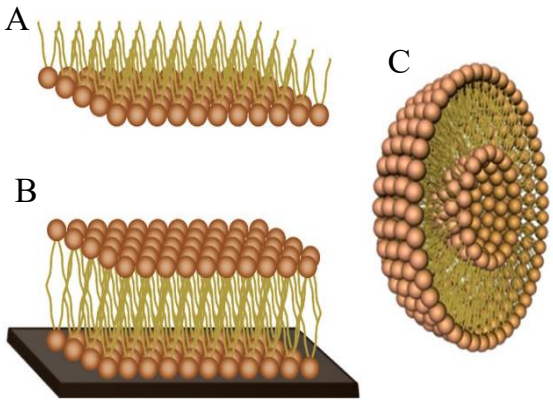

Figure 13: Schematic representation of membrane models: (A) lipid monolayer, (B) supported lipid bilayer, (C) liposome (Deleu *et al.*, 2014).

D. Molecular Dynamics as a tool to study the interaction

The experimental techniques studying the model membrane are numerous. Each technique uses a particular physical principle and gives a specific information on the membrane. As a whole, they are often combined with the aim to have a broader point of view on the interaction between bioactive molecules and the PPM. The experimental techniques can give two kinds of information, either the global effects of the molecule on the lipids or information at the molecular/atomistic level. *In silico* techniques such as Molecular Dynamics (MD) simulations are used to obtain molecular-specific information.

Molecular dynamics (MD) are a computational- and time-consuming technique simulating the evolution of a molecular system at an atomic scale. The system can be modelled in different ways. First, it can be represented by all the atoms of the system and the interactions between each atom are calculated, this is called the all-atom model. Second, the molecules can be composed of groups of neighbouring atoms with the same function regrouped in beads. In this case, the interactions between the beads are calculated. This simplification allows for the reduced need for computational power and thus for a shorter simulation time. This second type of simulation is called coarse grain model. Thirdly, a mix of the two previous model exists. When atoms interact with neighbour atoms of another molecules, all the atoms are modelled but when the interaction of atoms are intramolecular, they are modelled as a single unit or bead. This system is called united-atom model. This allows for a reduced need in computational power while keeping a good precision. This method was used in this thesis. An example of those models is given in Figure 14.

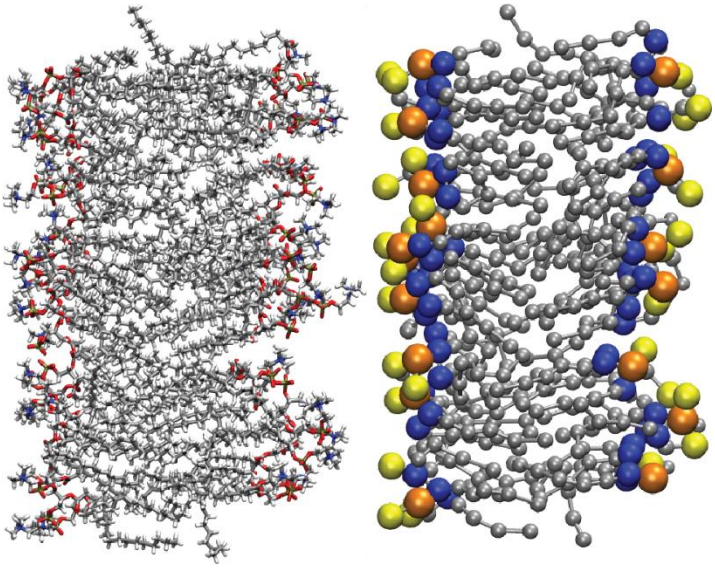

Figure 14: Representation of all-atom (on the left) and the MARTINI coarse grained (on the right) models.

To better simulate realistic conditions, the system is inserted into a box containing water molecules and periodic boundary conditions (PBC) are used to imitate a large system. The PBC take the initial water box and duplicate it periodically so that when an object passes through one side of the unit cell, it re-appears on the opposite side with the same velocity (Fig 15).

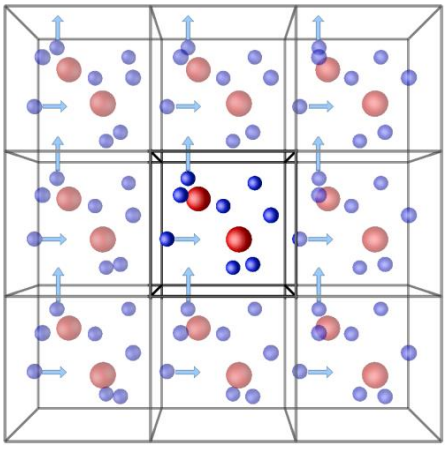

Figure 15: Schematic representation of periodic boundary conditions (PBC) (Central Michigan University).

The principle behind MD relies on the law of Newton (Eq. 1) to calculate the position of each atom at time $t+dt$.

Equation 1

$$F_i = m_i . a_i$$

By knowing the mass of atom i and the force applied to it, it is possible to calculate the acceleration of the atom from which the velocity $t+dt$ can be obtained. Once the velocity $t+dt$ is known, it can be coupled with the position t to determine the position $t+dt$. At each time-step, the trajectory which is composed of the position and velocity is calculated. The time-step

dt is generally of one or two femtoseconds. The succession of time-steps leads to a simulation that can reach nanoseconds and even microseconds if the machine is powerful enough.

The force F of Eq. 1 is calculated with Eq. 2 where U is the empirical potential energy and r the position.

Equation 2

$$F_i = \frac{-dU_i}{dr_i}$$

The potential energy must reflect the interaction of each atom with its neighbours. It must combine the intra- and interatomic interaction and bonded or nonbonded interaction (Fig. 16). The bonded interactions are composed of covalent bonds, dihedral bonds (torsional angles) and valence angle bends. The nonbonded interactions are mainly Van Der Waals and electrostatic interactions. The interactions are modelled by simplified functions (Fig. 16). The equations and parameters used to describe molecules and their interactions are described as forcefields.

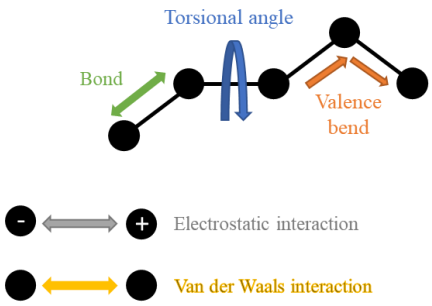

$$U_{pot} = \sum_{bonds} K_b(b - b_0)^2 \quad \text{Covalent bond}$$
$$+ \sum_{angles} K_\alpha(\alpha - \alpha_0)^2 \quad \text{Valence bend}$$
$$+ \sum_{torsion} \frac{V_n}{2}(1 + \cos[n\theta - \delta]) \quad \text{Torsional angle}$$
$$+ \sum_{ij} \frac{q_i q_j}{\epsilon r_{ij}} \quad \text{Electrostatic interaction}$$
$$+ \sum_{ij} \varepsilon[\left(\frac{Rmin_{ij}}{r_{ij}}\right)^{12} - \left(\frac{Rmin_{ij}}{r_{ij}}\right)^{6}] \quad \text{Van der Waals interaction}$$

Figure 16: Schematic representation of bonded and nonbonded interactions and their functions.

MD simulations enable a precise analysis of the system. In the case of bioactive molecules interacting with a lipid bilayer, it can namely determine the depth of insertion of the molecules into the bilayer and the hydrogen bonds between the molecules and the membrane.

OBJECTIVES

Current chemical herbicides are put under scrutiny for their adverse effects on the environment and human health and for their decreasing efficiency. It has led to the search of natural molecules more respectful for the environment using new molecular mechanisms of action.

The herbicidal properties of cinnamon and Java citronella essential oils have been shown in detail in the introduction section. In particular some of their main constituents such as CIN, CitO and CitA were shown to have the capacity to cause damages to *A. thaliana* (Dal Maso, Lins and Fauconnier, 2016). However, the molecular activities of those components are currently unknown. Since it appears that the cell membrane plays an important role in the interaction between the EO molecules and the plant, we assume that the PPM is one of their molecular targets and that their amphiphile nature helps them to insert into the lipid bilayer to change its properties.

This thesis aims at studying the relationships of the structure, activity and membrane interaction for CIN, CitO and CitA using complementary *in silico* and *in vitro* biophysical approaches. Since PPM are complex dynamic entities, their interaction with bioactive molecules is very difficult to study at the molecular level. For this reason, model membranes will be used in this study.

On the one hand, we have performed MD simulations to gain insight on the interaction of the three molecules at the molecular level. Physico-chemical parameters such as the rapidity and depth of the insertion as well as the stability of the molecules and the effects on the membrane properties are analysed.

On the other end, complementary *in vitro* experiments (ITC and Langmuir trough), giving global information on the interaction, were carried out to validate the *in silico* calculations. ITC gives the thermodynamic parameters for the interaction, while the Langmuir trough enables to explore a possible lipid specificity for the three molecules under investigation.

As a whole, this study will contribute to shed light on the hypothesis that PPM could be a molecular target for CIN, CitO and CitA in relation with their herbicidal effects.

MATERIALS AND METHODS

A. Chemicals

As mentioned above, we use model membranes mimicking PPM. For this, 1-palmitoyl-2-linoleoyl-sn-glycero-3-phosphocholine (PLPC), glucosylceramide and β-sitosterol were chosen to represent the PPM of *A. thaliana*. All the lipids were purchased from Avanti Polar Lipids, Inc. The lipids and lipidic derivatives are at all time kept from the light.

For this thesis, three major components of two EO were chosen based on a previous study demonstrating their efficacity as herbicidal molecules. Trans-cinnamaldehyde from the essential oil of *Cinnamomum zeylanicum* Blume (cinnamon) and (+)-citronellol and (+)-citronellal from *Cymbopogon winterianus* Jowitt (Java citronella) EOs. They were bought as well as all other chemicals from Sigma Aldrich. The EO main components are all kept from the light and CitA and CIN are stored at 4°C. CitO isn't heat-sensitive and doesn't require to be kept at lower temperature.

B. Molecular Dynamics simulations

Several steps are carried out in this approach. First, the input files such as the structure and topologies of molecules must be created or retrieved in databases. The forcefield has then to be chosen. They will be used to map out the system. Once the basis of the system is constructed, it is inserted inside a box which is filled with a solvent and ions if necessary. The system then undergoes an energy minimisation step which stabilises it by removing steric clashes and incorrect geometry. After that, two equilibration simulations are run where the molecules under investigation are kept under restraints for the solvent to equilibrate itself around them. The first equilibration brings the system to the desired temperature and volume while the second brings the system to the wanted pressure. Finally, the main production run is realised once all the parameters have been stabilised.

In this thesis, these steps were repeated two times. The first time to create and stabilise the membrane and the second time to create the interaction between the membrane and the EO components.

Simulations have been realised with GROMACS 5.0.2 in a Linux environment. Topologies of β-sitosterol, CIN, CitO and CitA were obtained with Automatic Topology Builder (Malde *et al.*, 2011). A PLPC topology derived from Berger Lipids forcefield (Berger, Edholm and Jähnig, 1997) and developed by Peter Tieleman's group was used (Tieleman, 2018). The forcefield used for the simulation is the united atom GROMOS 53a6 force field (Oostenbrink *et al.*, 2004).

Bilayers containing 102 PLPC molecules and 26 sitosterol molecules were generated and hydrated by using Memgen (Knight and Hub, 2015). The system was solvated with SPC water (Hermans *et al.*, 1984).

The membrane firstly underwent an energy minimization step followed by a 100 ps NVT equilibration and by a 1 ns NPT equilibration. The NVT equilibration enables the stabilisation of the temperature at an average of 298K by using the Nose-Hoover thermostat (Nosé, 1984; Hoover, 1985). The NPT equilibration stabilises the semi-isotropic pressure at an average of 1 bar by using the Parrinello-Rahman barostat (Parrinello and Rahman, 1981). A production run of 500 ns of the membrane was realised to stabilize the membrane.

After the stabilization of the membrane, thirteen herbicide molecules (lipid:EO component molar ratio of 10:1) distant of 0.8nm from each other and from the boundaries of the water box were inserted. The molecules were placed on one side of the membrane at 0.8nm from the PLPC phosphate.

The system then underwent a 100 ps NVT equilibration followed by a 100 ps NPT equilibration with the parameters established previously. During the equilibration, the molecules of interest were under position restraints. Finally, 100 ns production runs were performed.

Electrostatic interactions were treated by using the Particle Mesh Ewald (PME) method. A cut-off of 1nm was used for Van der Waals interactions. Bond lengths were upheld with the LINCS algorithm (Hess *et al.*, 1997). Trajectories were examined with GROMACS tools and FATSLIM (Buchoux, 2016) as well as with homemade scripts and were visually analysed with VMD (Humphrey, Dalke and Schulten, 1996). The results were laid out thanks to the program Grace (Stambulchik, 2015).

a. Molecular Dynamics analyses

The insertion of CIN, CitO and CitA were visualised using snapshots obtained with VMD at 94, 95 and 96ns respectively (Fig. 19, page 30). The time of the snapshots were chosen to better visualise the insertion. In this figure, PLPC, sitosterol and the bioactive molecules were represented but the solvent was omitted for the sake of clarity.

The graphs of transversal cut into the membrane were realised with the mean z coordinates of the mass centre of the thirteen bioactive molecules and of the PLPC phosphates (Fig. 21, p. 34). The phosphates are used to represent the hydrophilic head of the lipid. Their stability allows them to be used as reference for the position of the membrane.

The graphs of the mean distance between the molecules, the PLPC phosphates and the centre of the membrane were realised (Fig. 20, p. 32). The distance was calculated with the average of the position vectors of the centre of the EO components and average vectors of the position of the phosphates. This analysis was further developed by studying the distance between individual molecules and the centre of the membrane. For clarity sake, not all molecules were shown only those having different behaviour were presented in Figure 22 (page 36). The distance of the thirteen individual molecules can be found in Figure S1, S2 & S3 (see annexes).

To further investigate the insertion of CitO into the membrane, snapshots were acquired from VMD at different step of CitO penetration (Fig. 23, p. 37). The snapshots were taken at the very

beginning of the simulation, at 28ns and at 36ns. The water molecules were omitted for better visualisation. The mean distance between CitO molecules were also calculated for each snapshot with VMD.

The order parameter for the carbon tails of PLPC was calculated with Gromacs (Fig. 24, p. 38), using equation 4 where Θ is the instantaneous angle between the C–H bond vector and a reference axis (z-axis). The higher S_{CH} is, the more ordered the membrane is. Sitosterol molecules have an acyl chain too short to determine the order parameter (Vermeer *et al.*, 2007).

Equation 3

$$S_{CH} = \langle \frac{3\cos^2\Theta - 1}{2} \rangle$$

The hydrogen bonds between the EO components and constituents of the membrane were calculated with VMD (Table 1, p. 38). The H bonds are characterised by a bond between an electron donor and an electron acceptor with a distance of 3.2Å and an angle of 20°. The two parameters were chosen after testing several distances and angles because they gave the more relevant results. As one EO component showed a very small number of H bonds with the membrane before insertion, this value was subtracted from the average number of H bonds after insertion. The number of H bonds between CIN, CitA and CitO and the two types of lipids is shown in table 1. The number of bonds between PLPC and sitosterol in the presence of inserted molecules was obtained by subtracting the number of bonds present in the initial equilibrated membrane.

The thickness of the membrane was calculated using Fatslim (Fig. 25, p. 40). Fatslim works as such: firstly, the lipid molecule is simplified as being a polar head group and an acyl chain. The orientation of the lipid is determined by the calculation of the angle between the bilayer normal and the acyl chain vector. A subdomain is then defined as lipids having the same orientation and the distance between the lipids from one leaflet and the other is calculated, yielding the thickness of the domain. The thickness is given by region as a colour gradient where the darker colour represents a thicker membrane. The molecule positions were added onto the graphs thanks to a homemade script.

C. *In vitro* experiments

a. Liposomes preparation

For ITC, LUVs of approximately 100nm in diameter were used. To prepare the LUVs, small amounts of lipids (PLPC/sitosterol 80/20 molar ratio or PLPC/sitosterol/GluCer 60/20/20) were dissolved into chloroform:methanol (2:1 v/v) in a round-bottom flask covered with aluminium foil. A rotary evaporator was used to remove solvent under low pressure. The flask containing the lipidic film was then kept overnight under vacuum to remove solvent traces. The lipidic film was then hydrated with 10 mM TRIS - HCl buffer at pH 7 prepared from Milli-Q water.

The flask was kept at a temperature (~ 40 °C) well above the transition phase temperature of the lipid for at least 1 h and vortexed for 1-2 min every 10 min to form multilamellar lipid vesicles (MLVs). Then, the MLV suspension underwent 5 freeze-thaw cycles in liquid nitrogen and a water bath at 40°C respectively. In order to get LUVs, MLV suspension was then extruded 15 times through polycarbonate filters with a pore diameter of 100 nm. Before the ITC measurement, all solutions were thoroughly degassed by ultrasonication.

b. Isothermal Titration Calorimetry

ITC measures the heat emitted (exothermic reaction) or absorbed (endothermic reaction) when the bioactive molecules and the liposomes interact together. This is performed by determining the power required to maintain a constant temperature in regard to a reference solution (Fig. 17). The liposomes are titrated into a solution containing the EO component. The change in heat energy is recorded over time and its analysis enables the determination of enthalpy changes due to the interaction between the titrated and titrating solutions. Parameters like binding affinities, binding enthalpies, binding entropies and free Gibbs energy can be determined and give a complete thermodynamic description of binding processes and insight on the origin and nature (electrostatic or hydrophobic) of the interaction (Deleu *et al.*, 2014).

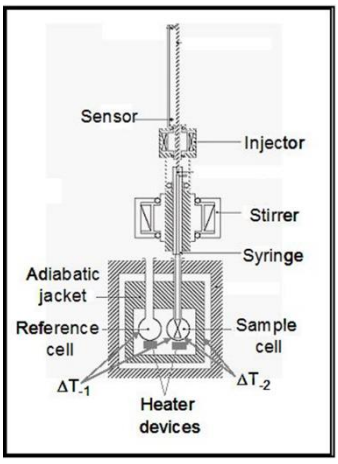

Figure 17: Scheme of an ITC (Martinez *et al.*, 2013).

ITC measurements were realised with a VP-ITC from Microcal (Microcal Inc., Northampton, MA, USA) at a constant temperature of 26°C. The sample cell contained 1.4565 mL of a solution of CIN, CitA or CitO (132 µM) dispersed from a DMSO stock solution into the same buffer as the LUV suspension. Reference cell was filled with mQ water. Small aliquots of LUV suspension were added to the sample cell with a software-controlled syringe. The first injection was 2 µL and was not considered for data treatment. It was followed by 28 successive additions of 10 µL spaced out with an interval of 600s. For the three molecules, a LUV concentration of 5 mM was used.

Data were analysed by software ORIGIN 7 (Originlab, Northampton, MA, USA) using the cumulative model as described in Razafindralambo *et al.* (2009) (Eq. 4).

Equation 4

$$\sum_{k=1}^{i} \delta h_k = \Delta H_D^{w \to b} V_{cell} C_A^0 \frac{K C_L^0}{1 + K C_L^0}$$

In this equation, δh_k is the heat produced after each injection which corresponds to the area of each peak on the heat flow. $\Delta H_D^{w \to b}$ is the difference in molar enthalpy originating from the transfer of the EO components from the aqueous phase to the lipidic bilayer, V_{cell} is the volume of the sample cell, C_A^0 and C_L^0 are respectively the total bioactive molecules and lipid concentration in the cell after i injections and K is the partition constant.

By fitting the measured cumulative heats in relation to the lipid concentration in the cell, K and $\Delta H_D^{w \to b}$ can be obtained. Equation 5 is then used to calculate the free Gibbs energy ($\Delta G_D^{w \to b}$) and the reaction entropy ($\Delta S_D^{w \to b}$).

Equation 5

$$\Delta G_D^{w \to b} = -RTln(KC_w) = \Delta H_D^{w \to b} - T\Delta S_D^{w \to b}$$

In this equation, R equals 8.31J.mol^{-1}.K^{-1}, T is the temperature in kelvin and C_w equals 55.5M.

The free Gibbs energy (ΔG) gives information on the favourability of the interaction. If ΔG is negative, it means that the binding is spontaneous and favourable. The absolute values of the enthalpy change (ΔH) and entropy change ($T\Delta S$) informs on the nature of the interaction. Indeed, Van der Waals interactions are enthalpy-driven processes while hydrophobic interactions are entropy-driven.

c. Langmuir trough

The Langmuir trough adsorption experiment measures the ability of a molecule to penetrate a monolayer membrane. To do so, a monolayer is first formed at the air/liquid surface by putting down lipids at the surface of the subphase. The bioactive molecules are then injected in the subphase. If possible, the molecules will penetrate the monolayer and increase the surface pressure. The pressure is measured by a Wilhelmy plate. A scheme of the Langmuir trough can be found in figure 18. The increased pressure resulting from the interaction, once analysed, gives the penetration kinetics and the extent of bioactive molecules that bind themselves to the monolayer. By plotting the maximal surface pressure increase as a function of the initial surface pressure, the maximal insertion pressure (MIP) and the differential Π0 (dΠ0) can be obtained.

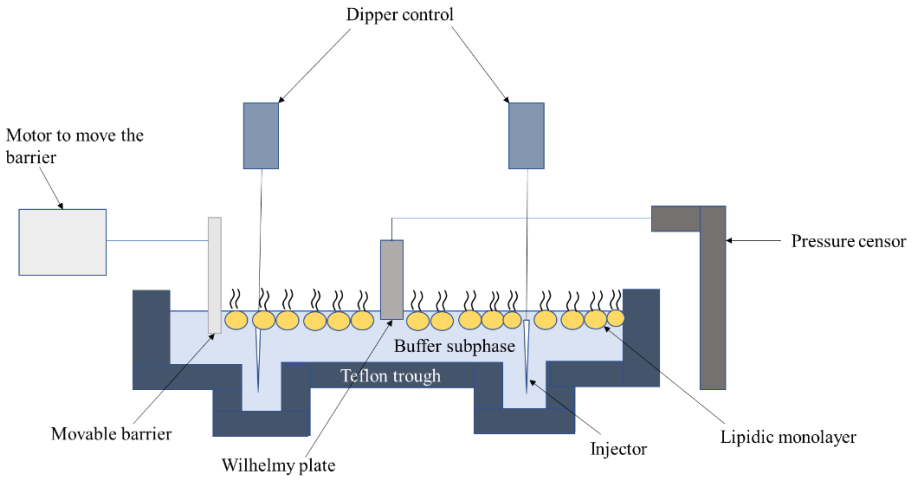

Figure 18: Scheme of the Langmuir trough.

The Langmuir trough experiment on the interaction of the molecules with the sitosterol monolayers were realised by Simon Dal Maso. Adsorption experiments were performed in a KSV Minitrough (Helsinki, Finland, 7.5 × 20 cm^2). The subphase was composed of Tris-HCl buffer at pH 7 prepared from Milli-Q water (~80 mL) with a constant temperature at 22.0 ± 1.0 °C. The subphase was continuously stirred with a magnetic stirrer. Pure PLPC or sitosterol molecules or a mix of the two lipids (PLPC/sitosterol 80/20 molar ratio) in chloroform:methanol (2:1 v/v) solvent, was spread at the air−water interface to reach the desired initial surface pressure. After 15 min of solvent evaporation and film stabilization, CitO, CitA or CIN in DMSO solution was injected underneath the preformed lipid monolayer. The final subphase concentration was 67.5 µM. Its adsorption to the lipid monolayer was followed by the increase in surface pressure.

As a control experiment, the same volume of pure DMSO was injected under the lipid monolayer with no observed change in the surface pressure. The Maximal Insertion Pressure (MIP) corresponds to the surface pressure beyond which no absorption can happen. It was obtained by linear regression of the plot ΔΠ vs Πi at the intersection with the *x* axis. The dΠ0 corresponds to the difference between ΔΠ0 which is the y-intercept of the linear regression of the ΔΠ vs Πi plot, and Πe which is the surface pressure increase at the equilibrium obtained in an independent experiment performed at the same CitA, CitO or CIN concentration but without lipids spread at the interface (Franche *et al.*, unpublished).

MIP informs on the capacity of the molecules to penetrate the membrane and stabilize themselves. $d\Pi_0$ denotes of the attraction or repulsion of the lipids for the interacting molecules. A positive $d\Pi_0$ means that the tested lipid has a favorable impact on the molecule adsorption. On the contrary, a negative value of $d\Pi_0$ signifies a repulsive effect of lipid on the molecule insertion. The MIP and $d\Pi_0$ uncertainties were calculated as described previously (Deleu *et al.*, 2019).

RESULTS

A. *In silico* biophysical assays

The interaction of 13 molecules of CIN, CitO, CitA with a lipidic bilayer composed of 102 PLPC molecules and 26 sitosterol molecules was analysed using MD. At the beginning of the simulation, the EO molecules were put in the water medium surrounding the lipidic bilayer. They were put at 0.8nm of the membrane and at 0.8nm of each other to avoid influencing the interaction. Their trajectory was simulated for 100 ns.

In Figure 19, it is clearly shown that the three EO components all penetrate the bilayer. Although molecules are present on both sides of the bilayer, they did not cross the bilayer but move to the other side of the box through the periodic boundary conditions.

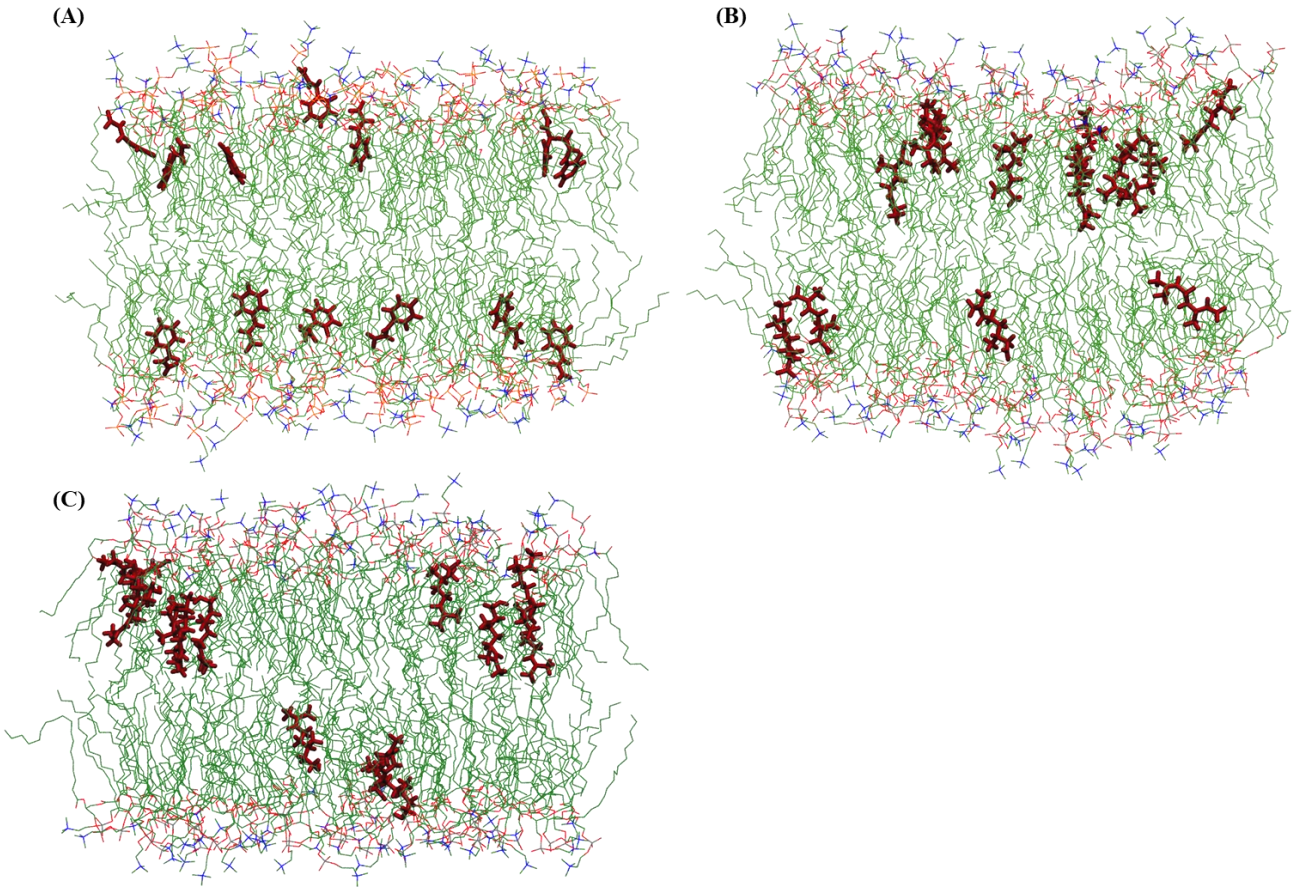

Figure 19: Snapshots after 100 ns of a 102 molecules PLPC and 26 molecules sitosterol bilayer with 13 molecules of (A) CIN (B) CitA and (C) CitO. For the sake of clarity, water molecules are omitted. Dark red: herbicidal molecules, green: carbon atoms, red: oxygen atoms, orange: phosphor atoms, blue: nitrogen atoms.

The depth and the time needed for the insertion have been analysed in different ways with a homemade script. First, we have checked the evolution of the mean distance from the centre of the membrane of both the EO molecules and of the lipids polar head (Fig. 20). Second, the insertion was represented by a transversal cut of the membrane where the evolution of the mean Z coordinates of both the mean mass centre of the bioactive molecules and of the PLPC phosphate groups (Fig. 21). Finally, the insertion was shown in more details as the evolution of the centre of mass of several individual bioactive molecules from the centre of the membrane

(Fig. 22). The three representations give insight into details that can differentiate the behaviour of the three different molecules.

Figure 20 confirmed that the three molecules are able to insert into the model membrane. The insertion depth is however greater for CitO and CitA (10Å from the membrane centre) as compared to CIN (at 12-13Å).

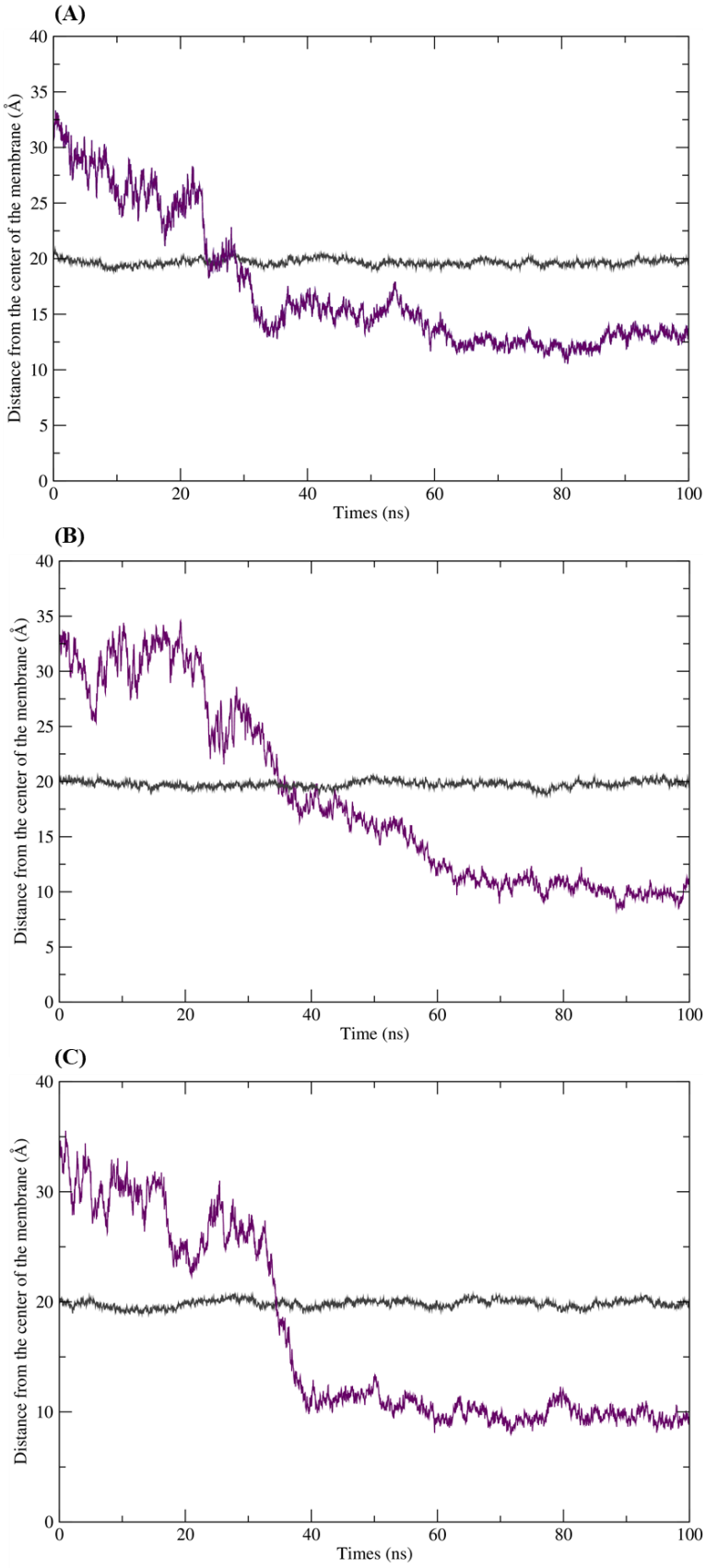

Figure 20: Evolution of the distance (in Angstroms) of the membrane composed of PLPC and sitosterol and of (A) CIN, (B) CitA and (C) CitO compared to the mass centre. Dark grey: mean distance between the mass centre of phosphate atoms of the PLPC molecules and the membrane centre, purple: mean distance between the mass centre of herbicidal molecules and the centre of the membrane.

This difference is also noticed when looking at the evolution of the mean Z coordinates of the both the mass centre of each EO component and that of the lipid phosphate groups, representing a transversal cut of the system (Figure 21). If CitA (Fig.21B) can stably penetrate the bilayer after 40ns, CIN appears to have a less stable and shallower membrane penetration. Fluctuations in the position of both CIN and the phosphate group of PLPC are observed, during 60ns of the simulation time (Fig. 21A). This indicates that the interaction of CIN with the membrane surface is less stable, the molecules appearing to go in and then out of the membrane, inducing a perturbation of the lipid polar heads. CitO inserts stably and deeply after 40ns as for CitA and seems to have an intermediate effect on the position of the lipid phosphate groups (Fig. 21C). Hence, the deeper insertion of CitA and CitO as compared to CIN is confirmed.

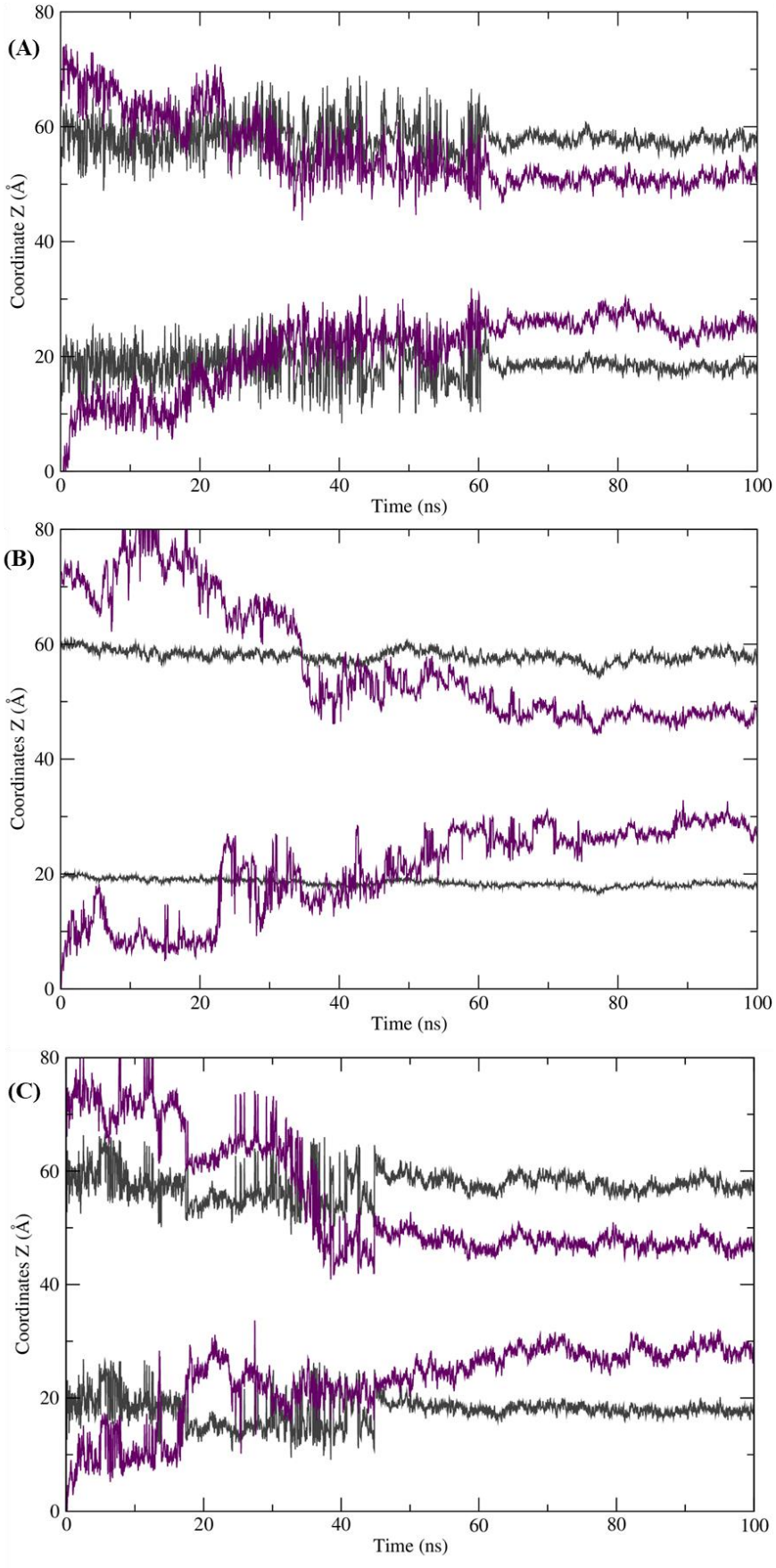

Figure 21: Transversal cut of PLPC and sitosterol bilayer in the presence of (A) CIN (B) CitA and (C) CitO. Dark grey: mean z coordinates of the mass centre of phosphate atoms of the PLPC molecules, purple: mean z coordinates of the mass centre of herbicidal molecules.

From figures 22, S1, S2 and S3, the behaviour of individual molecules is analysed. In figure 22, three types of behaviour were selected, molecules inserting before 20ns, between 20 and 50ns and after 50ns.

For CIN, five molecules penetrate the membrane before 20ns, six between 20ns and 50ns and two after 50ns (Fig. 22A, S1). The relatively even partition informs us that CIN molecules tend to penetrate the membrane individually. The Figure S1 confirms this and shows that CIN appears to stay near the interface, rarely reaching the centre of the membrane. Interestingly, one CIN molecule gets outside the membrane before re-entering 15ns later (Fig. 22A). This seems to confirm the less stable interaction of CIN with the lipids.

As for CIN, CitA molecules enter the membrane individually with one molecule inserting before 20ns, eight between 20 and 50ns and four after 50ns (Fig. 22B). Once within the membrane, they seem to fluctuate deeper in the bilayer. During the last 20 ns, some molecules seem to reach the centre of the membrane (Fig. S2).

The penetration of CitO in the membrane is uneven as shown in Figure S3 where two CitO enter the bilayer before 20ns, ten between 20 and 40ns and one molecule after 40ns. Interestingly, we also observe that CitO molecules tend to insert as clusters (Fig S3). Once inserted, CitO and CitA stay inside the membrane during the whole simulation (Fig. 22C, S3) and seem to be more stably inserted as compared to CIN.

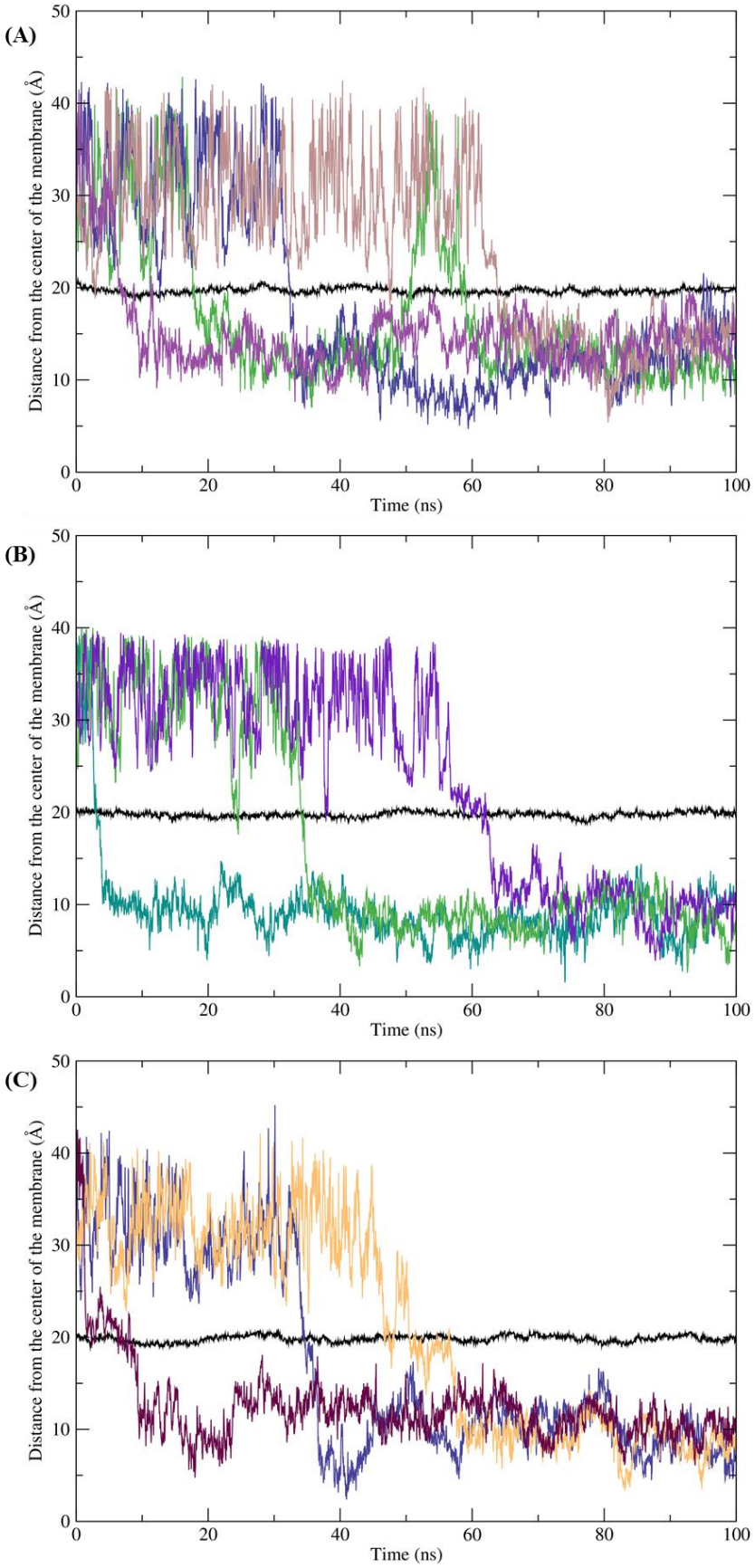

Figure 22: Evolution of the distance in Angstrom between mass centre of the membrane and 13 molecules of (A) CIN, (B) CitA and (C) CitO. For the sake of clarity, not all molecules are represented. Black: mean distance between the mass centre of phosphate atoms of the PLPC molecules and the membrane, colours: distance between the mass centre of herbicidal molecules and the mass centre of the membrane.

The clustered insertion of CitO was further investigated in Figure 23. This figure depicts the different steps of CitO penetration, confirming that the molecules gather before entering the bilayer. At the beginning of the simulation (Fig. 23A), the mean distance between CitO molecules is 18.3Å. After 28ns, the mean distance is 9.9Å (Fig. 23B). After 36ns, the mean distance between the bioactive molecules is 8.5Å (Fig. 23C). Although the molecules tend to penetrate the membrane as a cluster, individual molecules can also enter the membrane.

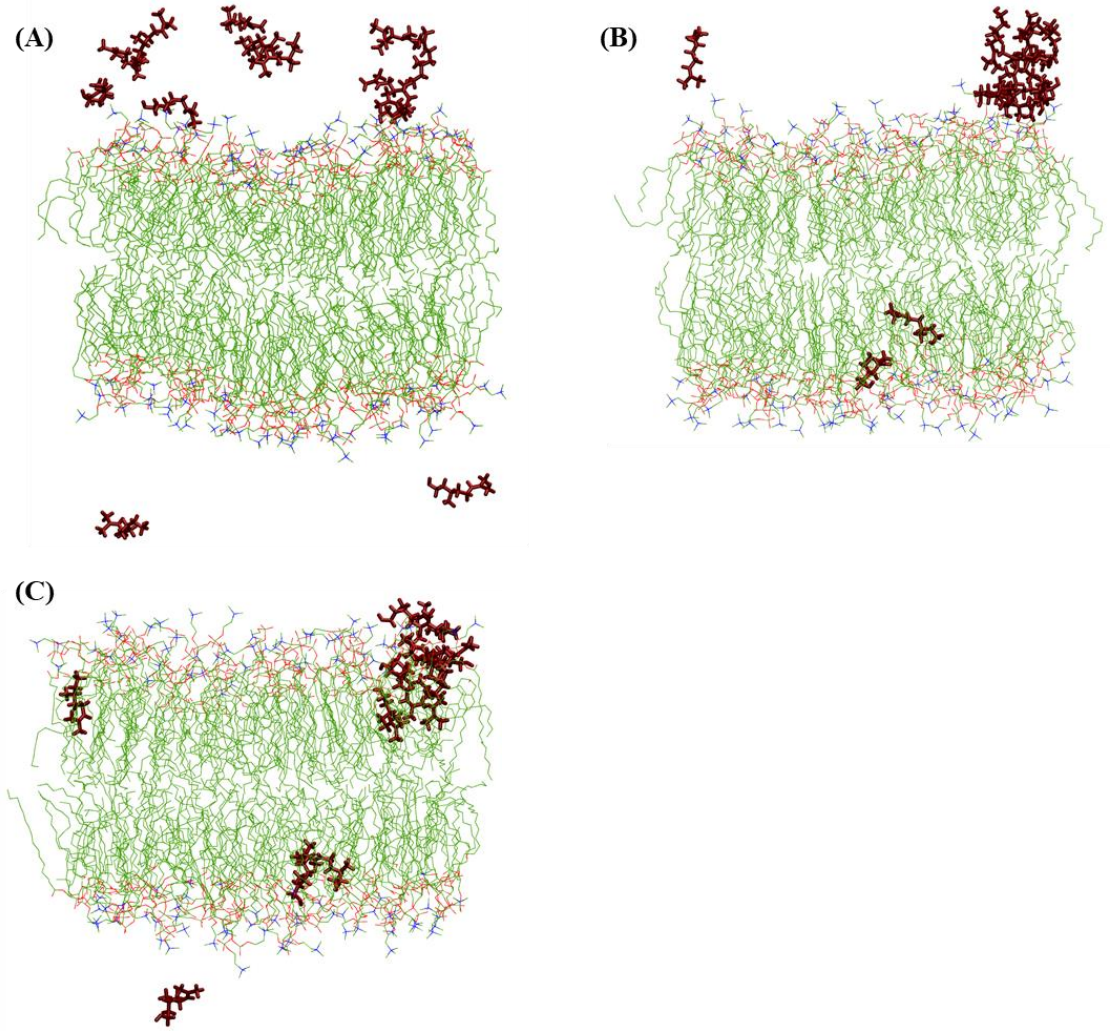

Figure 23: Snapshots of CitO taken (A) at the beginning of the simulation, (B) after 28ns and (C) after 36ns. For the sake of clarity, water molecules are omitted. Dark red: herbicidal molecules, green: carbon atoms, red: oxygen atoms, orange: phosphor atoms, blue: nitrogen atoms.

At the end of the 100 ns run, we have analysed different physico-chemical parameters of the membrane, such as the order parameter, the hydrogen bonds formed and the thickness of the membrane.

PLPC has two acyl chains, the palmitoyl and the linoleoyl acyl chain. The palmitoyl chain is saturated while linoleoyl chain has two double bonds. As expected, the order parameter of the two PLPC acyl chains appears very different (Fig. 24), due to the double bonds present in the linoleoyl chain at position 9 and 12, rendering the chain less ordered.

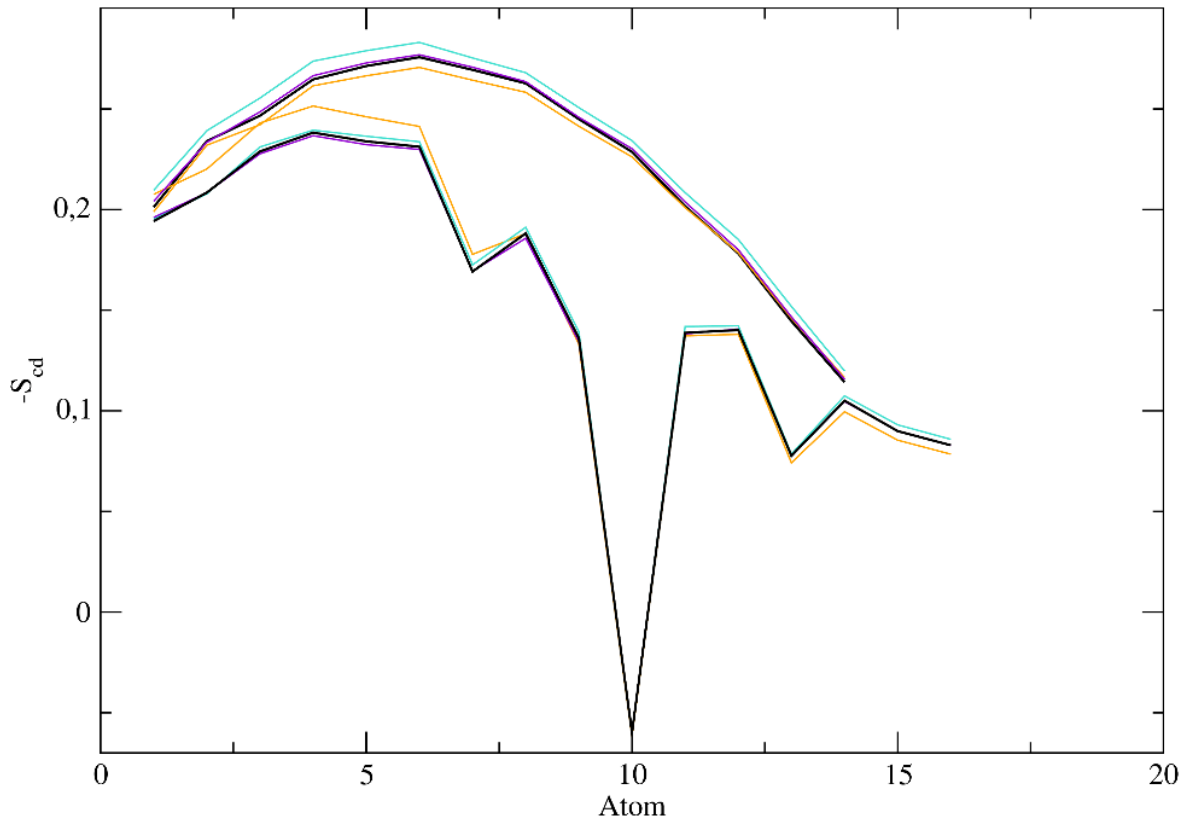

Figure 24: The order parameter of the palmitoyl (upper curves) and linoleoyl (lower curves) PLPC chains. In black: membrane only, in orange: membrane containing CIN, in purple: membrane containing CitA, in blue: membrane containing CitO.

CIN shows a slight ordering of the linoleoyl chain of the carbon atoms at proximity of the interface while CitO slightly orders the palmitoyl acyl chain all along the chain. For CitA, no obvious change can be seen for either chain.

Table 1 shows the mean number of hydrogen bonds created by the interaction of each EO component with the lipids.

Table 1: Mean number of hydrogens bonds between three EO components and the membrane and and the loss of hydrogen bonding of the lipids due to the interaction with CitO, CitA or CIN.

	Molecules/ PLPC & sitosterol	**Molecules/PLPC**	**Molecules/Sitosterol**	**PLPC/Sitosterol**
CitO	4,91	3,71	1,2	-0,85
CitA	0,39	0,00	0,39	-0,98
CIN	0,30	0,00	0,30	-0,95

We observed that CitO forms significantly much more hydrogens bonds with the membrane than the two other molecules. It interacts preferentially with PLPC molecules as compared to sitosterol. It also decreases the number of H bonds between PLPC and sitosterol.

CitA and CIN form very few H bonds that are solely made with sitosterol. CitA creates slightly more bonds than CIN. The insertion of CitA decreases the number of bonds between PLPC and sitosterol more than the insertion of CIN and CitO. Despite CitO making more links with the membrane, its insertion diminishes the number of links between PLPC and sitosterol the least out of the three EO components.

We have also analysed the evolution of the thickness of the membrane, at the beginning (Fig. 25, upper panels) and at the end of the simulation (Fig. 25, lower panels) in the presence of the individual EO components.

From figure 25A, CIN does not seem to affect significantly the thickness of the membrane. We also noticed that CIN molecules are inserted in the membrane where it is thinner.

CitA and CitO have a different behaviour. The insertion of CitA does not seem to depend on the thickness of the membrane and it globally makes the bilayer thicker. This effect is significantly more pronounced for CitO where the whole membrane thickens after its insertion. Interestingly, CitO molecules appear to insert as cluster as compared to the other two components, in agreement with the data from Figure 22C and S3.

As a whole, the data from MD simulations suggest that CIN inserts into the membrane less deeply and less stably than CitA or CitO. Besides, CitO seems to have more impact on the lipid bilayer that CitA.

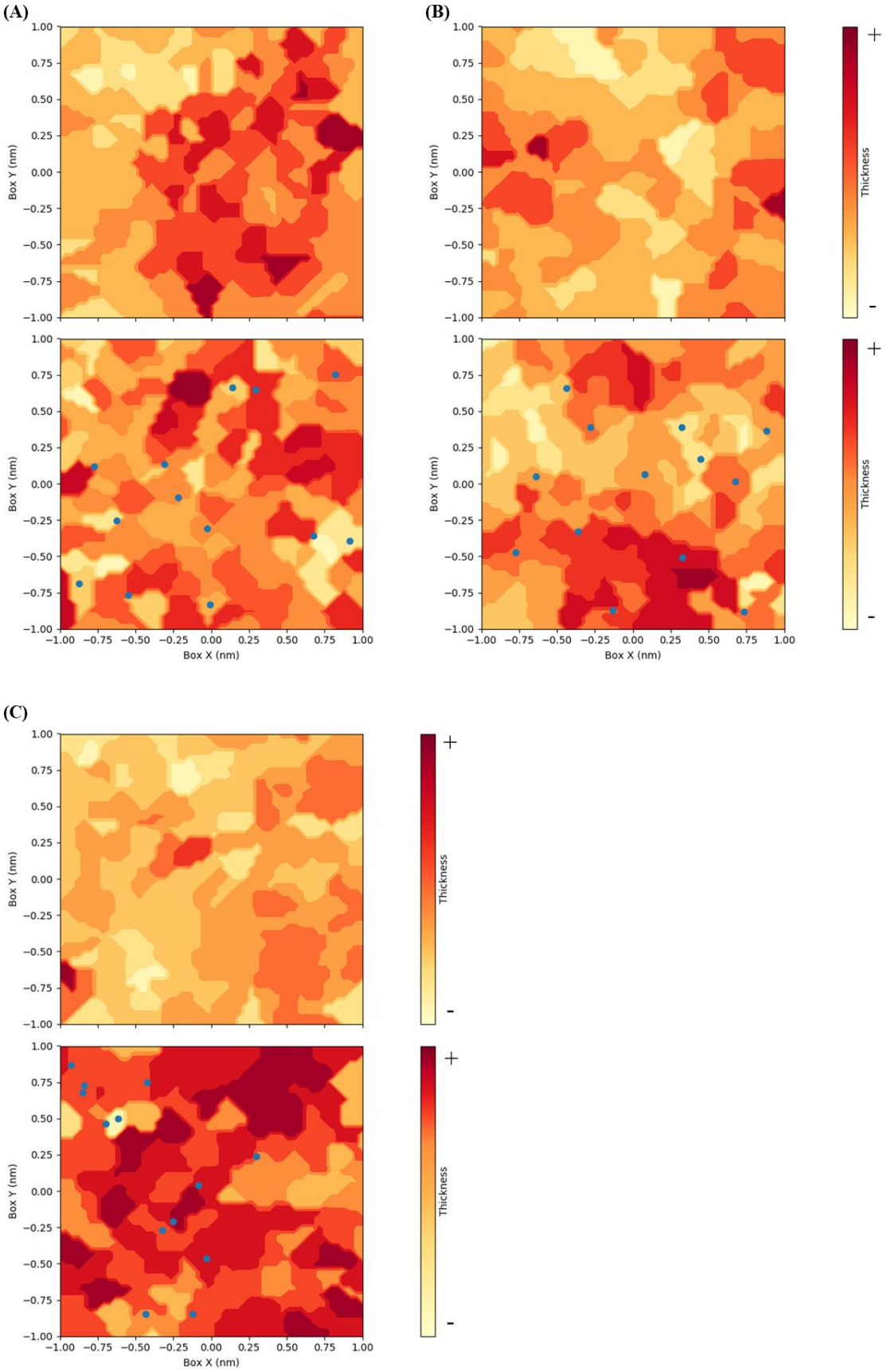

Figure 25: Thickness of the membrane at the beginning and at the end of the simulation in presence of (A) CIN, (B) CitA and (C) CitO. Upper panels: the thickness at the beginning of the simulation, lower panels: thickness at the end of the simulation. Blue dots: EO components.

B. *In vitro* biophysical assays

a. Thermodynamic characterisation of the interaction

ITC enables the study of the partition of the EO components into the lipid bilayer and to characterize the thermodynamics of the interaction. In those experiments, the heat emitted or absorbed following the interaction of the EO components with the liposomes will be recorded over time. As time goes on, more and more EO molecules will have interacted with the lipid vesicles, less will be left to interact and thus the heat emitted or absorbed will decrease. Typical raw data are shown on Figures 26 and 27. The faster the heat decreases the more the molecules are reactive and the higher the affinity is. In addition to the affinity, ITC also gives information on the interaction enthalpic and entropic energies from which the type of interaction can be discussed.

ITC analyses were carried out on PLPC/sitosterol and PLPC/sitosterol/GluCer liposomes. PLPC/sitosterol vesicles were chosen to be compared to MD data. A sphingolipid, glucosylceramide, was added to the lipid composition to have a more realistic PPM model.

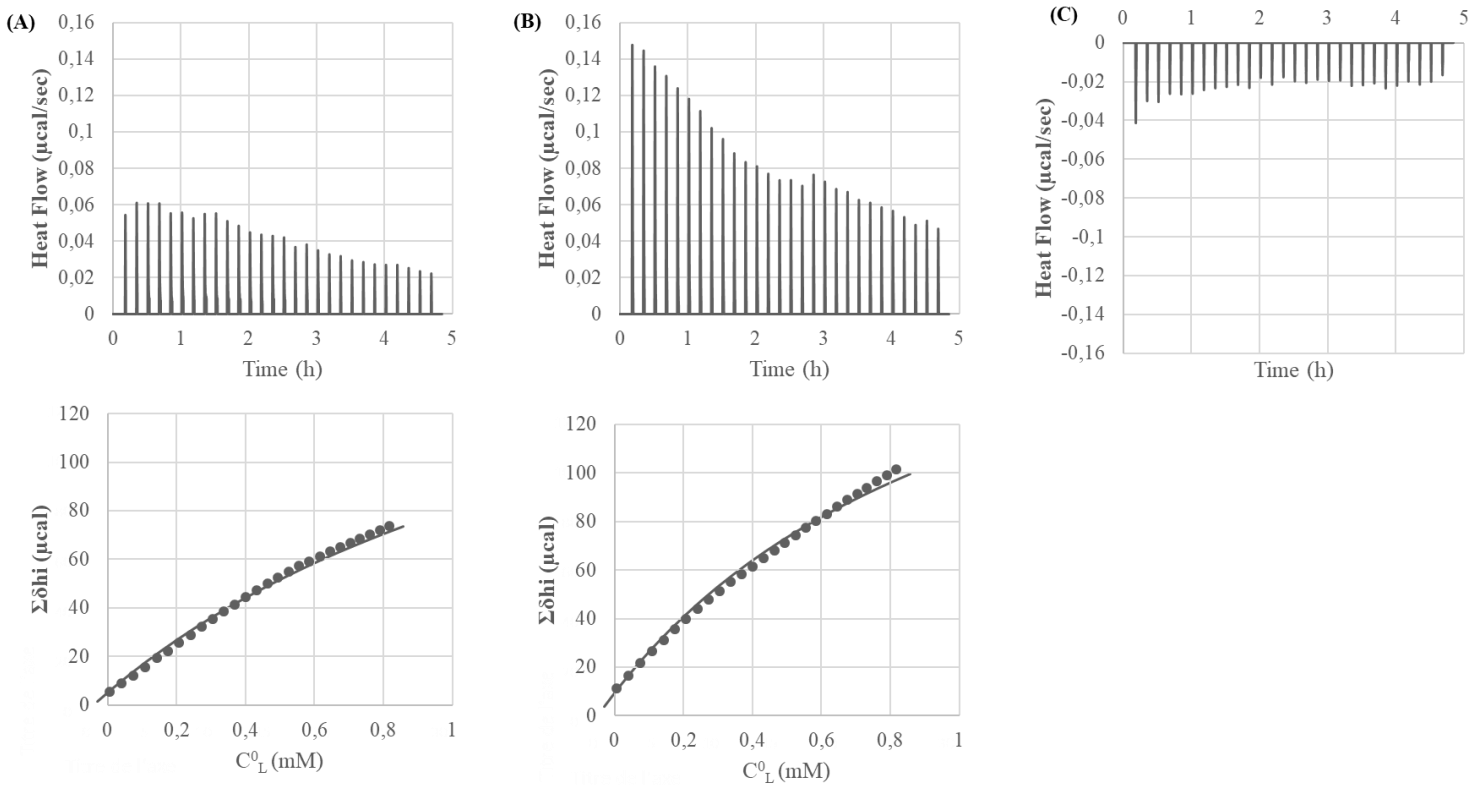

Figure 26 : Upper panels: raw data from ITC experiment. Each peak corresponds to a single injection of 10µL of PLPC/sitosterol LUV suspension of mM into a 132µM solution of (A) CitA, (B) CitO and (C) CIN at 26°C. LUV suspensions and herbicides solution were buffered at pH 7,4 with Tris-HCl. Lower panels: cumulative heats of binding (Σδhi) as a function of lipid concentration in the cell (C^0_L). No fitting could be realised with cinnamaldehyde due to an absence of interaction. N = 3

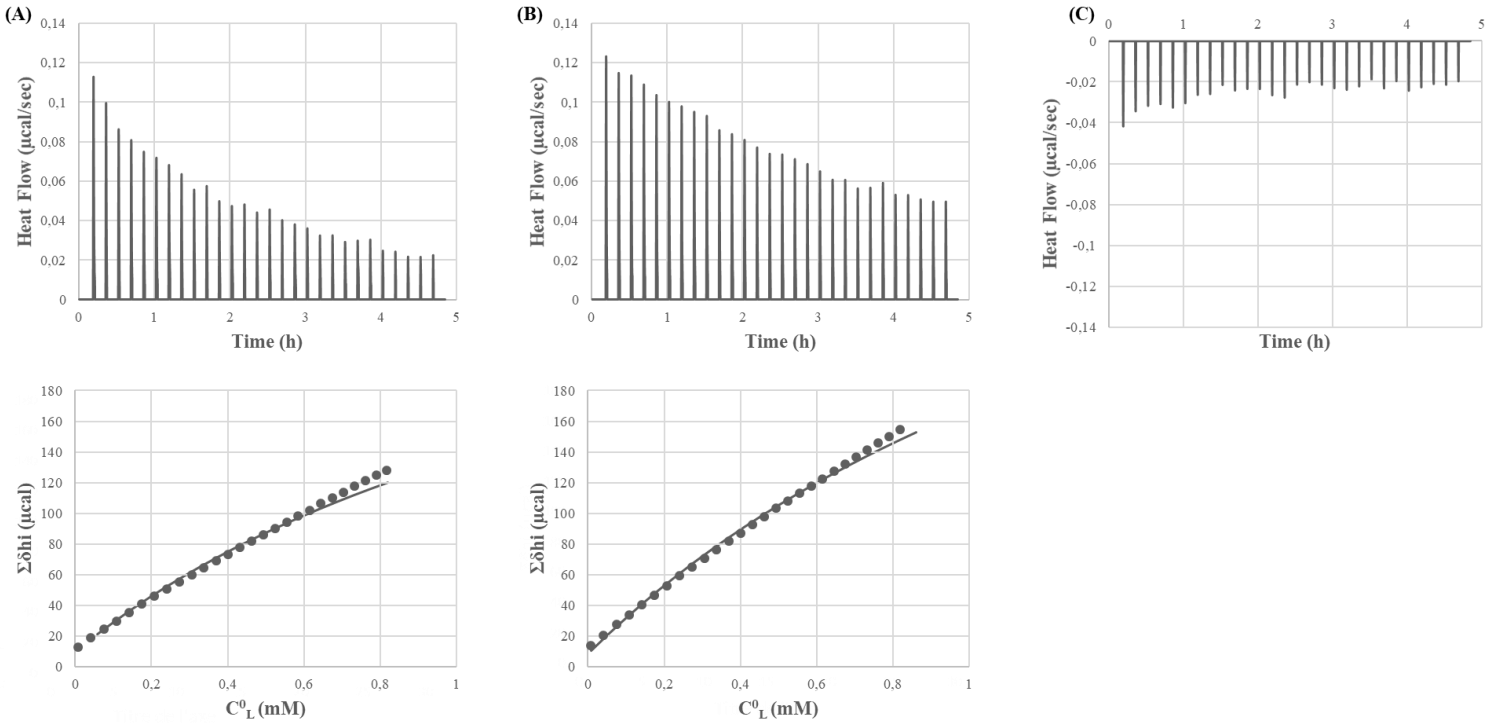

Figure 27: Upper panels: raw data from ITC experiment. Each peak corresponds to a single injection of 10µL of PLPC/sitosterol/GluCer LUV suspension of mM into a 132µM solution of (A) CitA, (B) CitO and (C) CIN at 26°C. LUV suspensions and herbicides solution were buffered at pH 7,4 with Tris-HCl. Lower panels: cumulative heats of binding (Σδhi) as a function of lipid concentration in the cell (C^0_L). No fitting could be realised with cinnamaldehyde due to an absence of interaction. N=3

The raw data for the two lipid compositions (Fig. 26 & 27) show that CitA and CitO display a gradual decrease of the positive heat flow signal over time representative of an interaction between the EO components and the liposomes while no decrease can be observed with CIN. Therefore, it can be hypothesised that no interaction occurs between CIN and the model membranes.

From the fitting curves, the thermodynamic parameters were extrapolated for CitO and CitA (Tables 2 and 3): the affinity (K), the enthalpic energy (ΔH), the entropic energy (TΔS) and the total energy (ΔG) of the binding were calculated.

Table 2 indicates that the binding of CitA or CitO is spontaneous ($\Delta G < 0$), endothermic ($\Delta H > 0$) and is led by a positive change of entropy ($\Delta S > 0$). The affinity for the binding is slightly higher for CitA than CitO.

Table 2 : Thermodynamic parameters characterizing the interactions of herbicidal molecules with PLPC/sitosterol LUVs.

Natural compounds	K (mM^{-1})	$\Delta H_D^{W \rightarrow D}$ ($kj.mol^{-1}$)	$T\Delta S_D^{W \rightarrow D}$ ($kj.mol^{-1}$)	$\Delta G_D^{W \rightarrow D}$ ($kj.mol^{-1}$)
Citronellal	0.03 ±0.00	5.13 ±0.64	21.62 ±0.34	-16.53 ±0.93
Citronellol	0.01 ±0.01	5.05 ±0.52	23.28 ±0.50	-18.47 ±0.46

The reaction of CitO and CitA with PLPC/sitosterol/GluCer bilayer is also spontaneous ($\Delta G < 0$), endothermic ($\Delta H > 0$) and denotes a positive change of entropy ($\Delta S > 0$) (Table 3). The affinity is similar for the two EO components.

Table 3 : Thermodynamic parameters characterizing the interactions of herbicidal molecules with PLPC/sitosterol/GluCer LUVs.

Natural compounds	K (mM^{-1})	$\Delta H_D^{W \rightarrow D}$ ($kj.mol^{-1}$)	$T\Delta S_D^{W \rightarrow D}$ ($kj.mol^{-1}$)	$\Delta G_D^{W \rightarrow D}$ ($kj.mol^{-1}$)
Citronellal	0.02 ±0.00	9.65 ±2.24	25.93 ±1.25	-16.28 ±1.17
Citronellol	0.01 ±0.01	10.17 ±0.98	27.22 ±0.71	-17.04 ±0.30

When comparing Tables 2 and 3, the affinity is not significantly different while the enthalpic and entropic energies are higher for the PLPC/sitosterol/GluCer bilayer. In both cases, the absolute value of entropy change is higher than the one of enthalpy change, indicating that the binding is entropy driven, i.e. hydrophobic. This is probably due to the transfer of the hydrophobic chain of CitA or CitO from the water to the hydrophobic core of the liposomes. This is supported by the fact that there is no obvious difference between the thermodynamic parameters of CitA and CitO, having the same hydrophobic tail.

b. Specificity of the interaction

The Langmuir trough was used to investigate a potential lipid specificity and to possibly differentiate the mechanism of lipid interaction between CIN, CitO and CitA. In those experiments, the adsorption of the molecule of interest to a lipid monolayer spread at the air-water interface is followed. Adsorption experiments with PLPC, β-sitosterol and PLPC/ β-sitosterol monolayers were performed for the three EO components.

The raw data of the adsorption experiments can be seen in Figure 28 where CitA and CitO but not CIN are able to adsorb to any lipid monolayer. This is in agreement with the ITC data.

Figure 28C also shows that the equilibrium state is reached faster for CitA and CitO into β-sitosterol monolayers.

The adsorption of CitO in PLPC and the PLPC/sitosterol monolayers appears to be peculiar. Indeed, it shows a rapid increase of the surface pressure just after the injection followed by a rapid decrease (Fig. 28A and B). One hypothesis is that this phenomenon is due to the rapid evaporation after injection of CitO.

In the case of β-sitosterol monolayer, the decrease is less rapid (Fig. 28C), suggesting that another phenomenon could occur, such as removal of lipid molecules from the monolayer to the subphase. This hypothesis is further supported by the fact that at higher initial surface pressure of β-sitosterol (above 15mN/m), there is a decrease of the surface pressure with time, to values lower than the initial pressure (Fig. 29).

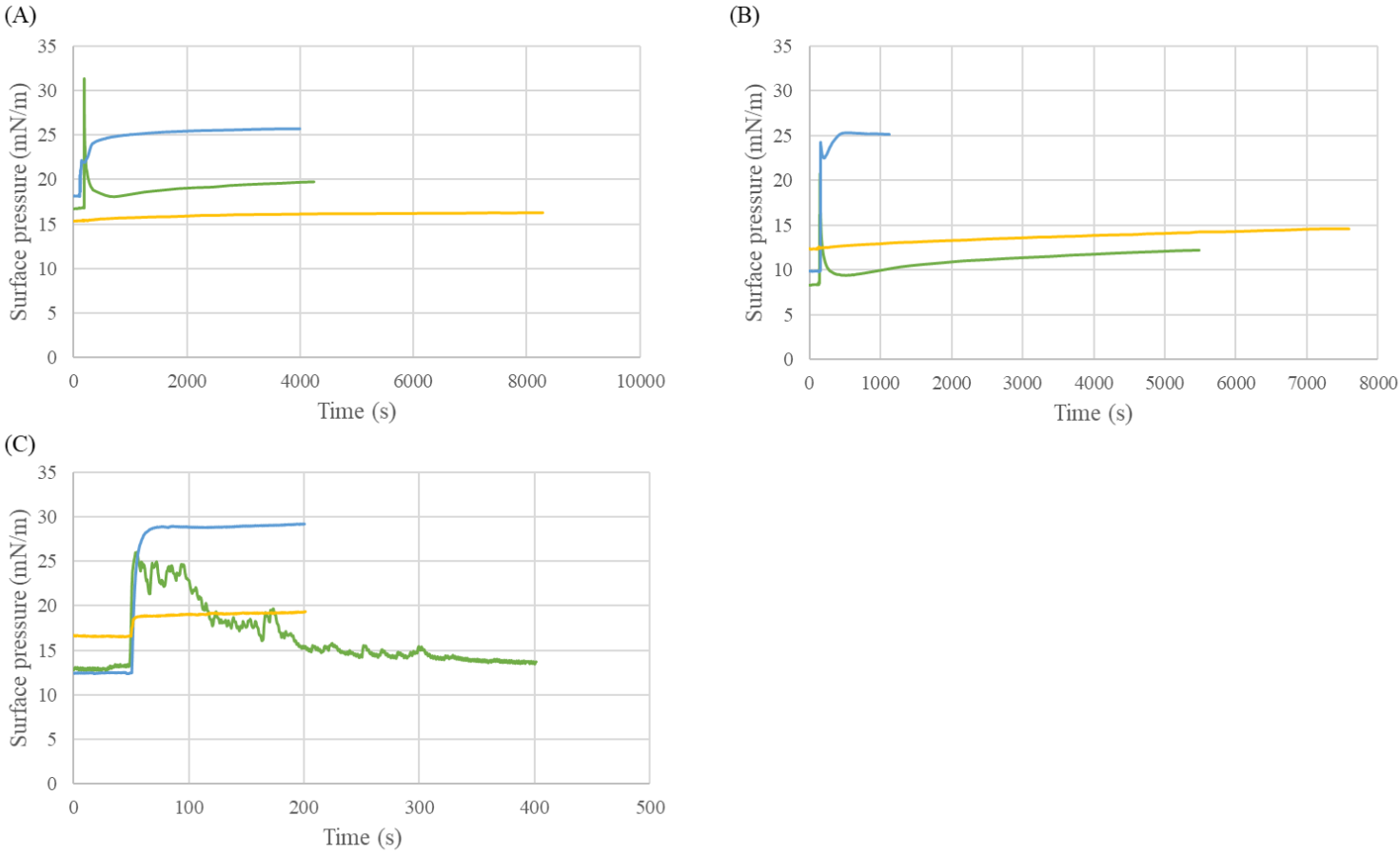

Figure 28: Evolution of the surface pressure with time of three components of EO in (A) PLPC (B) PLPC/sitosterol and (C) Sitosterol monolayer. In green: CitO, in blue: CitA and in orange: CIN.

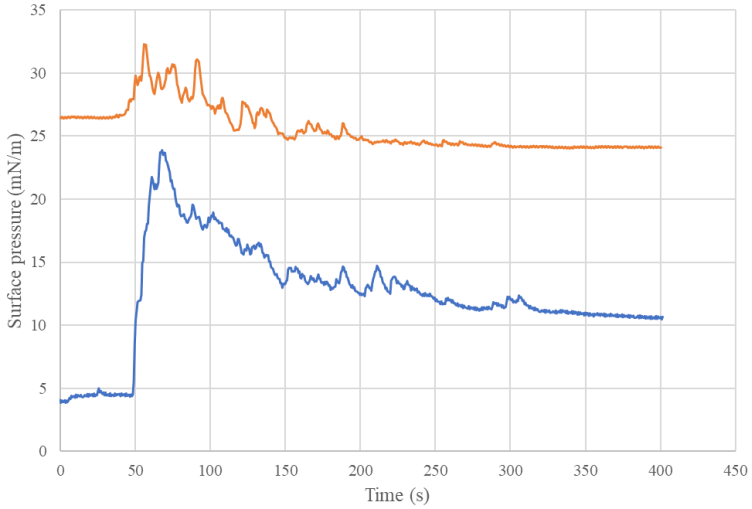

Figure 29: Adsorption of CitO into a β-sitosterol monolayer. Evolution of the surface pressure with time: in blue at an initial surface pressure of 4mM/m and in orange at an initial surface pressure of 26mN/m.

Plots of the surface pressure variation at the equilibrium versus the initial surface pressure (Fig. 30) were used to obtain the binding parameters, i.e. the Maximal Insertion Pressure (MIP) and $d\Pi_0$, shown in figure 31. MIP is linked to the penetration power of EO main components while $d\Pi_0$ shows the attractiveness or repulsiveness of the lipids for the bioactive molecules.

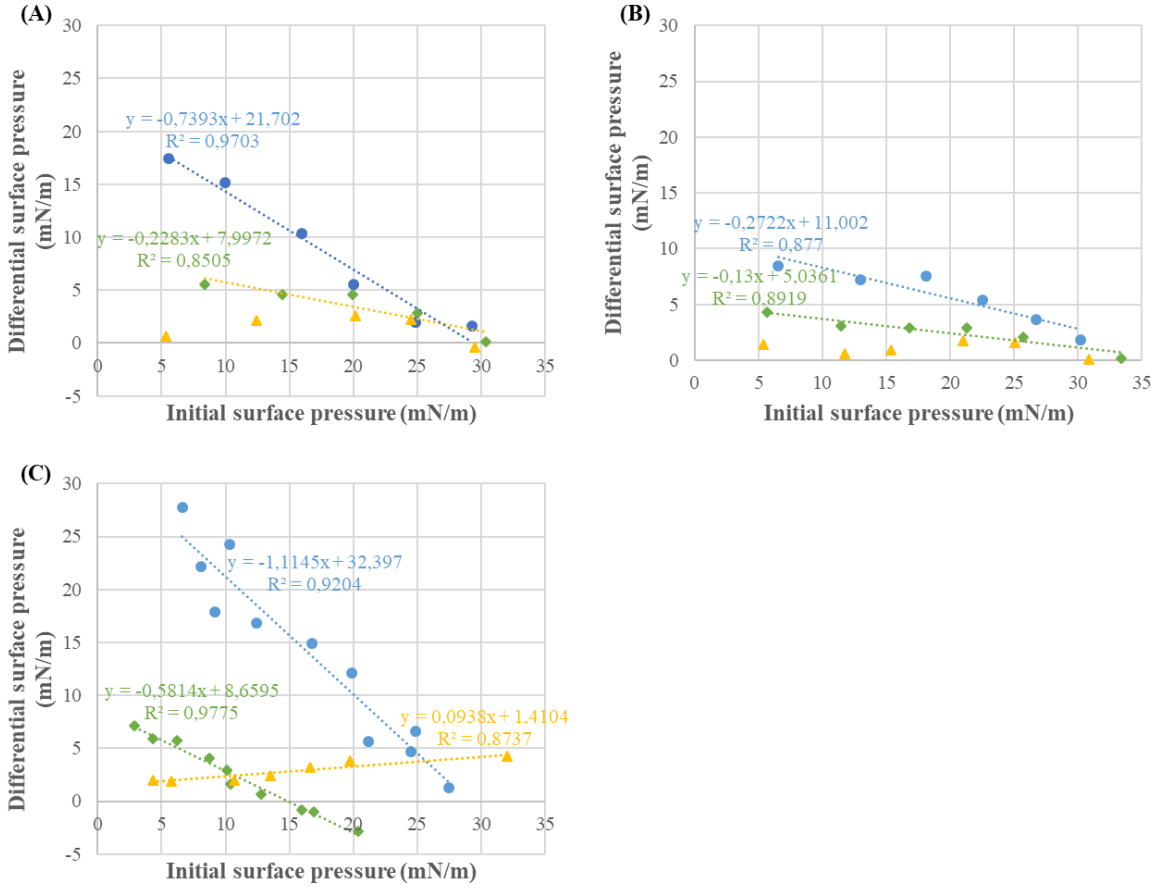

Figure 30: Evolution of the differential surface pressure monolayer with the initial surface pressure of herbicidal molecules citronellal (●), citronellol (◊) and cinnamaldehyde (Δ) into lipid monolayers: (A) PLPC/sitosterol (B) PLPC and (C) Sitosterol.

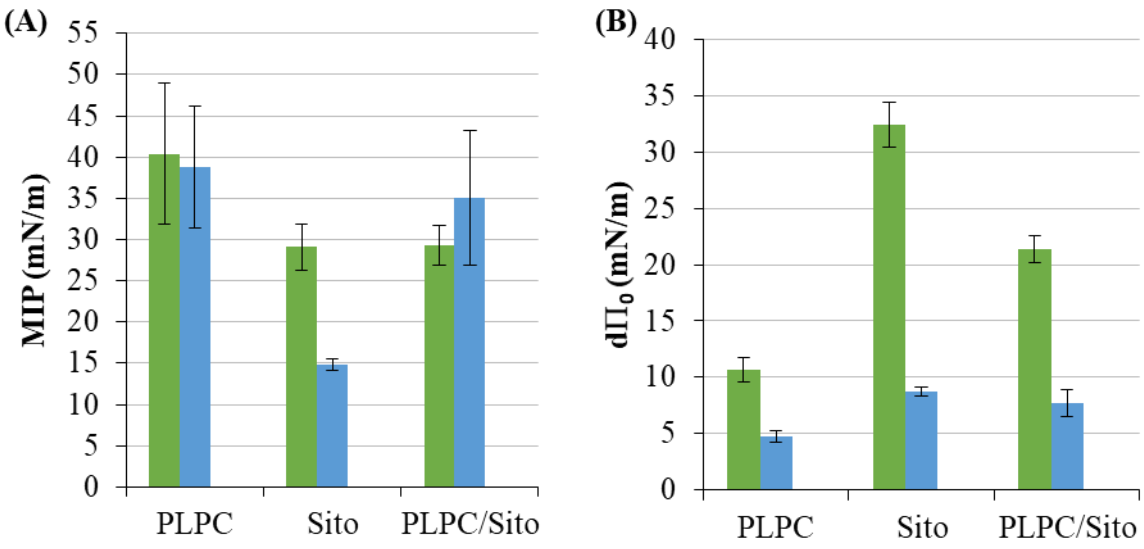

Figure 31: Adsorption of CitA (green) and CitO (blue) into lipid monolayers: PLPC, PLPC/sitosterol and Sitosterol. (A) Maximal insertion pressure (MIP) and (B) differential ⎡⎤0 (d⎡⎤0) values. For CIN, MIP and d⎡⎤0 were not quantifiable.

For the binary lipid composition, CitO and CitA have a MIP close or higher than the lateral pressure supposed to prevail in natural membranes (30-35mN/m) (Marsh, 1996) (Fig. 31). It suggests that CitA and CitO but not CIN can insert into natural PPM. The positive values of $d\Pi_0$ indicate that the PPM lipids have an attractive effect on CitA and CitO. This effect is higher for CitA than CitO.

Individual lipid monolayers and especially that of β-sitosterol show also a higher attractive effect on CitA than on CitO. However, in terms of penetration power (MIP), PLPC seems to be more favorable to the penetration and stabilization of both molecules. The physical state of the monolayer which is more rigid in the presence of β-sitosterol can hence have an influence on the insertion behavior of the two molecules.

DISCUSSION

This master thesis investigated the molecular mechanisms of action of three EO components possessing herbicidal properties, namely CitO, CitA and CIN. The herbicidal effects of the three molecules have been studied both in a previous study realised by the host lab (Dal Maso, Lins and Fauconnier, 2016) and in literature (Chaimovitsh *et al.*, 2017; Chotsaeng, Laosinwattana and Charoenying, 2018). The mechanisms involved in the toxicity are supposed to affect either the energy metabolism such as photosynthesis and/or involve ROS production. Electrolyte leakage is often observed, indicating that the integrity of the cell membrane is affected. These studies suggest that the cell membrane could be a target through which phytotoxicity is exerted.

The plasma membrane is also one of the action sites described for the antimicrobial activities of EOs, so we tested whether the individual compounds of the two EOs selected, cinnamon and Java citronella EO, were able to interact with a model membrane mimicking PPM. Our complementary *in silico* and *in vitro* biophysical approaches indicated that CitO and CitA can stably interact with plant lipids, while CIN has no stable interaction with the membrane.

For CIN, MD approaches suggested that it could not interact stably with the model membrane over 100ns but can however penetrate at the level of the lipid polar heads and disturb them. During the simulation, the molecules penetrated the membrane individually. One molecule was also shown to get out of the membrane before re-entering it. Experimentally, no interaction could be noticed in ITC or Langmuir monolayer assays. The timescale of the MD simulations (nanoseconds) being far from the *in vitro* timescale (seconds to minutes) could be insufficient to observe more CIN molecules getting out of the membrane. Nevertheless, we cannot rule completely out that the volatile nature of CIN could also be involved in the absence of interaction with the membrane. In the literature, CIN has been described as interacting with monolayers of lipids mimicking bacterial membrane (Nowotarska *et al.*, 2014). The different results might be explained by the fact that CIN could have an affinity for bacterial lipids and not for plant lipids that are quite different in their physico-chemical properties.

On the other hand, CitO and CitA have comparable affinities for plant lipids, since the thermodynamic parameters for their interaction with PLPC/sitosterol liposomes are similar. The interaction is entropy-driven, due to the fact that their alkyl chain can interact with the lipid hydrocarbon chains, as observed in the MD simulations. When looking at the effects of the individual lipids, we observed that PLPC has an attractive effect for both molecules, especially for CitA. Sitosterol has an even more pronounced effect on the latter. However, we noticed a peculiar behaviour of CitO in the presence of sitosterol monolayer. There is a rapid increase of surface pressure in the seconds after the injection of CitO, followed by a gradual decrease of the pressure. If the evaporation of CitO could be responsible for this observation, another hypothesis can be put forward: CitO could be able to remove sterol molecules from the lipidic film. This is supported by the fact that CitO is able to displace cholesterol molecules from its phospholipid partners (Lange *et al.*, 2009). This effect is referred to as cholesterol activation. We can assume that CitO could have the same effect on sitosterol, having a similar structure as cholesterol.

MD simulations allow to deepen the analysis of the effect of CitO and CitA on the membrane. First, both molecules insert deeper within the membrane than CIN. Moreover, CitA and even more CitO thicken the membrane after their insertion. A very notable difference between the two EO components is their mechanism of penetration. CitO tends to penetrate the membrane as clustered molecules while CitA inserts individually. CitO also forms more H-bonds with the membrane constituents, notably with sitosterol. This confirms again that the interaction of CitO and the sterols are particular as compared to CitA.

If CitO and CitA were shown to interact with model PPM, they do not exert their phytotoxic effect by simply destroying the membrane, since a previous study has shown that the two molecules do not induce leakage of fluorescent probes when interacting with PLPC/sito liposomes (Dal Maso, Lins, Fauconnier, 2016). This is in agreement with the fact that the antimicrobial effects of some terpenes such as γ-terpinene or p-cymene are not necessarily linked to significant membrane perturbation (Cristani *et al.*, 2007). The latter should be dependent on the lipidic composition and net surface charge (Cristani *et al.*, 2007). Subtler mechanisms for membrane perturbations, such as thickening of the membrane, as observed here in MD simulations or modification of lipid nano- or microdomains, involved in signalling processes, could also be involved in the toxic effect observed *in planta*. This was already suggested for other natural molecules such as surfactin (Henry *et al.*, 2011). The latter is a bacterial amphiphile molecule that is able to elicit the plant defences by acting on the lipid part of the membrane.

For CIN, other molecular mechanisms can be assumed. This molecule as well as molecules belonging to the phenylpropanoid family such as eugenol, were shown to be agonists and ligands of mammal membrane ion channels, namely transient receptor potential Ankyrin 1 (TRPA1) and transient receptor potential vanilloid 1 (TRPV1) (Namer *et al.*, 2005; Tsagareli *et al.*, 2010; Chung *et al.*, 2014). A yet-to-discover plant membrane protein could be involved in toxic effects of CIN on plants.

CIN’s inability to interact with the membrane might be caused by its lower hydrophobicity compared to CitO and CitA. The difference observed between CitO and CitA may be due to their difference in structure. The alcohol function of CitO might be the driving force between the clustering of the molecules in the MD simulations and the higher number of H bonds.

CONCLUSION AND PERSPECTIVES

In conclusion, the PPM could be one site of action for CitO and CitA but not for CIN, that could be related to their different chemical structure. The membrane activity of the formers is not leakage, but probably a subtler effect on membrane domains or on membrane properties. The mechanism of action of the latter might be to target membrane protein.

Further studies on the effects of CitO and CitA on membrane micro/nanodomains and on the physical state of the lipids should be carried out. An important class of plant lipids has not been investigated in this study, namely GIPC sphingolipids (Cacas *et al.*, 2016). They are however not commercially available for the moment. Another important issue for a better understanding of the toxic effects of EO compounds at the molecular level is to study their effects on the plant gene expression and metabolic pathways.

In the prospect of using the three molecules as bioherbicide, more information still needs to be gathered on the effect of the EO components on plants *in vivo*. To do so, the study of synergistic/antagonistic herbicidal effects between the different components of essential oils need to be studied, as well as the penetration kinetics of these compounds into the different tissues of the leaf together with the development of formulations allowing slow and controlled release (Maes, Bouquillon and Fauconnier, 2019). All those aspects should help to better understand the effects of the individual components of cinnamon and Java citronella EOs at the molecular level. This should lead to an optimal formulation of a natural herbicide targeting multiple and/or other molecular pathways as compared to conventional herbicides.

BIBLIOGRAPHY

Araújo-filho, J. V. De *et al.* (2018) ‘Effects of Eucalyptus citriodora essential oil and its major component, citronellal, on Haemonchus contortus isolates susceptible and resistant to synthetic anthelmintics’, *Industrial Crops & Products*. Elsevier, 124(July), pp. 294–299. doi: 10.1016/j.indcrop.2018.07.059.

Bartke, N. and Hannun, Y. A. (2009) ‘Bioactive sphingolipids: metabolism and function’, *Journal of Lipid Research*, 50(Supplement), pp. S91–S96. doi: 10.1194/jlr.r800080-jlr200.

Beckie, H. J. *et al.* (2011) ‘A decade of herbicide-resistant crops in Canada’, *Canadian Journal of Plant Science*, 86(4), pp. 1243–1264. doi: 10.4141/p05-193.

Berger, O., Edholm, O. and Jähnig, F. (1997) ‘Molecular dynamics simulations of a fluid bilayer of dipalmitoylphosphatidylcholine at full hydration, constant pressure, and constant temperature’, *Biophysical Journal*, 72(5), pp. 2002–2013. doi: 10.1016/S0006-3495(97)78845-3.

Bouyahya, A. *et al.* (2019) ‘Essential oils of Origanum compactum induce membrane permeability, disturb cell membrane, and suppress quorum-sensing phenotype in bacteria’, *Journal of Pharmaceutical Analysis*. Elsevier. doi: 10.1016/J.JPHA.2019.03.001.

Brown, D. A. and London, E. (2002) ‘Functions of Lipid Rafts in Biological Membranes’, *Annual Review of Cell and Developmental Biology*, 14(1), pp. 111–136. doi: 10.1146/annurev.cellbio.14.1.111.

Buchoux, S. (2016) ‘Fast Analysis Toolbox for Simulations of Lipid Membranes’. Available at: https://pythonhosted.org/fatslim/.

Burt, S. (2004) ‘Essential oils: Their antibacterial properties and potential applications in foods - A review’, *International Journal of Food Microbiology*, 94(3), pp. 223–253. doi: 10.1016/j.ijfoodmicro.2004.03.022.

Cacas, J.-L. *et al.* (2016) ‘Revisiting Plant Plasma Membrane Lipids in Tobacco: A Focus on Sphingolipids’, *Plant Physiology*, 170(1), pp. 367–384. doi: 10.1104/pp.15.00564.

Cahyono, E. *et al.* (2014) ‘Analysis Of The Enantiomers Ratio Of Citronellal From Indonesian Citronella Oil Using Enantioselective Gas Chromatography’, *Malaysian Journal of Fundamental and Applied Sciences*, 9(2), pp. 62–66. doi: 10.11113/mjfas.v9n2.84.

Cangussu, A. S. R. *et al.* (2017) ‘Phytotoxic effects of essential oils in controlling weed species Digitaria horizontalis and Cenchrus echinatus’, *Biocatalysis and Agricultural Biotechnology*. Elsevier Ltd, 12(August), pp. 59–65. doi: 10.1016/j.bcab.2017.08.016.

Casares, D., Escribá, P. V. and Rosselló, C. A. (2019) ‘Membrane lipid composition: Effect on membrane and organelle structure, function and compartmentalization and therapeutic avenues’, *International Journal of Molecular Sciences*, 20(9). doi: 10.3390/ijms20092167.

Castillo-Morales, R. M. *et al.* (2019) ‘Mitochondrial affectation, DNA damage and AChE inhibition induced by Salvia officinalis essential oil on Aedes aegypti larvae’, *Comparative Biochemistry and Physiology Part C: Toxicology & Pharmacology*. Elsevier, 221, pp. 29–37. doi: 10.1016/J.CBPC.2019.03.006.

Cavalieri, A. and Caporali, F. (2010) ‘Effects of essential oils of cinnamon, lavender and peppermint on germination of Mediterranean weeds’, *Allelopathy Journal*, 25(2), pp. 441–452.

Chaimovitsh, D. *et al.* (2017) ‘Herbicidal Activity of Monoterpenes Is Associated with Disruption of Microtubule Functionality and Membrane Integrity’, *Weed Science*. 2016/11/04. Cambridge University Press, 65(1), pp. 19–30. doi: DOI: 10.1614/WS-D-16-00044.1.

Chotsaeng, N., Laosinwattana, C. and Charoenying, P. (2018) ‘Inhibitory effects of a variety of aldehydes on Amaranthus tricolor l. And echinochloa crus-galli (L.) beauv.’, *Molecules*, 23(2). doi: 10.3390/molecules23020471.

Chung, G. *et al.* (2014) ‘Activation of transient receptor potential ankyrin 1 by eugenol’, *Neuroscience*, 261, pp. 153–160. doi: 10.1016/j.neuroscience.2013.12.047.

Cristani, M. *et al.* (2007) ‘Interaction of Four Monoterpenes Contained in Essential Oils with Model Membranes: Implications for Their Antibacterial Activity’, *Journal of Agricultural and Food Chemistry*, 55(15), pp. 6300–6308. doi: 10.1021/jf070094x.

Dal Maso, S., Lins, L. and Fauconnier, M.-L. (2016) ‘Étude de l’interaction d’huiles essentielles avec des membranes végétales modèles par des approches bio-physiques complémentaires : relation structure-fonction dans la perspective de développement de bio-herbicides’, *Unpublished*.

Deleu, M. *et al.* (2014) ‘Complementary biophysical tools to investigate lipid specificity in the interaction between bioactive molecules and the plasma membrane: A review’, *Biochimica et Biophysica Acta - Biomembranes*. Elsevier B.V., 1838(12), pp. 3171–3190. doi: 10.1016/j.bbamem.2014.08.023.

Deleu, M. *et al.* (2019) ‘Linoleic and linolenic acid hydroperoxides interact differentially with biomimetic plant membranes in a lipid specific manner’, *Colloids and Surfaces B: Biointerfaces*. Elsevier, 175(November 2018), pp. 384–391. doi: 10.1016/j.colsurfb.2018.12.014.

Dilworth, L. L., Riley, C. K. and Stennett, D. K. (2017) ‘Plant Constituents: Carbohydrates, Oils, Resins, Balsams, and Plant Hormones’, *Pharmacognosy*. Academic Press, pp. 61–80. doi: 10.1016/B978-0-12-802104-0.00005-6.

Dufourc, E. J. (2008) ‘Sterols and membrane dynamics’, *Journal of Chemical Biology*, 1(1–4), pp. 63–77. doi: 10.1007/s12154-008-0010-6.

Eslahi, H., Fahimi, N. and Sardarian, A. R. (2017) ‘Chemical composition of Essential Oils’, 4(2), pp. 119–171.

FAO (2009) ‘Global agriculture towards 2050’, *High Level Expert Forum-How to feed the world 2050*, pp. 1–4. doi: http://www.fao.org/fileadmin/templates/wsfs/docs/Issues_papers/HLEF2050_Global_Agriculture.pdf.

FAO (2017) 'The future of food and agriculture: trends and challenges', *Food and Agriculture Organization of the United Nations*. doi: 10.4161/chan.4.6.12871.

Franche, A. *et al.* (no date) ‘Amphiphilic azobenzenes: antibacterial activities and biophysical investigation of their interaction with bacterial membrane lipids’, *Wiley-VCH*.

Furt, F., Simon-Plas, F. and Mongrand, S. (2010) 'Lipids of the Plant Plasma Membrane', *Plant Cell Monographs*. Edited by A. S. Murphy, W. Peer, and B. Schulz. doi: 10.1007/978-3-642-13431-9_20.

Gnankiné, O. and Bassolé, I. L. H. N. (2017) ‘Essential oils as an alternative to pyrethroids’ resistance against anopheles species complex giles (Diptera: Culicidae)’, *Molecules*, 22(10). doi: 10.3390/molecules22101321.

Green, J. M. (2014) ‘Current state of herbicides in herbicide-resistant crops’, *Pest Management Science*, 70(9), pp. 1351–1357. doi: 10.1002/ps.3727.

Gronnier, J. *et al.* (2018) ‘Divide and Rule: Plant Plasma Membrane Organization’, *Trends in Plant Science*. Elsevier Current Trends, 23(10), pp. 899–917. doi: 10.1016/J.TPLANTS.2018.07.007.

Henry, G. *et al.* (2011) ‘The bacterial lipopeptide surfactin targets the lipid fraction of the plant plasma membrane to trigger immune-related defence responses’, *Cellular Microbiology*, 13(11), pp. 1824–1837. doi: 10.1111/j.1462-5822.2011.01664.x.

Hermans, J. *et al.* (1984) ‘A consistent empirical potential for water–protein interactions’, *Biopolymers*, 23(8), pp. 1513–1518. doi: 10.1002/bip.360230807.

Hess, B. *et al.* (1997) ‘LINCS: A Linear Constraint Solver for molecular simulations’, *Journal of*

Computational Chemistry, 18(12), pp. 1463–1472. doi: 10.1002/(SICI)1096-987X(199709)18:12<1463::AID-JCC4>3.0.CO;2-H.

Hoover, W. G. (1985) 'Canonical dynamics: Equilibrium phase-space distributions', *The American Physical Journal*, 31(3), pp. 1695–1697. doi: 10.1007/BF00419952.

Hu, W. *et al.* (2019) 'Antibacterial activity and mechanism of Litsea cubeba essential oil against methicillin-resistant Staphylococcus aureus (MRSA)', *Industrial Crops and Products*. Elsevier, 130(December 2018), pp. 34–41. doi: 10.1016/j.indcrop.2018.12.078.

Huang, F. *et al.* (2019) 'Membrane damage mechanism contributes to inhibition of trans-cinnamaldehyde on Penicillium italicum using Surface-Enhanced Raman Spectroscopy (SERS)', *Scientific Reports*. Springer US, 9(1), pp. 1–10. doi: 10.1038/s41598-018-36989-7.

Huang, Y. and Ho, S. H. (1998) 'Toxicity and antifeedant activities of cinnamaldehyde against the grain storage insects, Tribolium castaneum (Herbst) and Sitophilus zeamais Motsch.', *Journal of Stored Products Research*, 34(1), pp. 11–17. doi: 10.1016/S0022-474X(97)00038-6.

Humphrey, W., Dalke, A. and Schulten, K. (1996) 'VMD: Visual Molecular Dynamics', *Journal of Molecular Graphics*, 14, pp. 33–38. doi: 10.1016/0263-7855(96)00018-5.

Kalemba, D. and Kunicka, A. (2003) 'Antibacterial and Antifungal Properties of Essential Oils', *Current Medicinal Chemistry*, 10(10), pp. 813–829. doi: 10.2174/0929867033457719.

Kang, J. *et al.* (2019) 'Antibacterial and anti-biofilm activities of peppermint essential oil against Staphylococcus aureus', *Lwt*. Elsevier, 101(August 2018), pp. 639–645. doi: 10.1016/j.lwt.2018.11.093.

Kaur, S. *et al.* (2011) 'Citronellol Disrupts Membrane Integrity by Inducing Free Radical Generation', *Zeitschrift für Naturforschung. C, Journal of biosciences*. doi: 10.5560/ZNC.2011.66c0260.

Khare, P. *et al.* (2019) 'Impact of essential oils of E. citriodora, O. basilicum and M. arvensis on three different weeds and soil microbial activities', *Environmental Technology & Innovation*. Elsevier, 14, p. 100343. doi: 10.1016/J.ETI.2019.100343.

Kiran, S. *et al.* (2017) 'Assessment of toxicity and biochemical mechanisms underlying the insecticidal activity of chemically characterized Boswellia carterii essential oil against insect pest of legume seeds', *Pesticide Biochemistry and Physiology*. Academic Press, 139, pp. 17–23. doi: 10.1016/J.PESTBP.2017.04.004.

Knight, C. J. and Hub, J. S. (2015) 'MemGen: A general web server for the setup of lipid membrane simulation systems', *Bioinformatics*, 31(17), pp. 2897–2899. doi: 10.1093/bioinformatics/btv292.

Lange, Y. *et al.* (2009) 'Activation of membrane cholesterol by 63 amphipaths', *Biochemistry*, 48(36), pp. 8505–8515. doi: 10.1021/bi900951r.

Laosinwattana, C., Wichittrakarn, P. and Teerarak, M. (2018) 'Chemical composition and herbicidal action of essential oil from Tagetes erecta L. leaves', *Industrial Crops and Products*. Elsevier, 126(October), pp. 129–134. doi: 10.1016/j.indcrop.2018.10.013.

Lim, S. and Shin, S. (2009) 'Effects of citronellol and thymol on cell membrane composition of Candida albicans', *Korean Journal of Pharmacognosy*.

Maes, C., Bouquillon, S. and Fauconnier, M.-L. (2019) 'Encapsulation of Essential Oils for the Development of Biosourced Pesticides with Controlled Release: A Review', *Molecules*, 24(14), pp. 1–17. doi: 10.3390/molecules24142539.

Malde, A. K. *et al.* (2011) 'An Automated Force Field Topology Builder (ATB) and Repository: Version 1.0', *Journal of Chemical Theory and Computation*, 7, pp. 4026–4037.

Markham, J. E. and Jaworski, J. G. (2007) 'Rapid measurement of sphingolipids from Arabidopsis

thaliana by reversed-phase high-performance liquid chromatography coupled to electrospray ionization tandem mass spectrometry', *Rapid Communications in Mass Spectrometry*, 21, pp. 1304–1314. doi: 10.1002/rcm.

Marsh, D. (1996) 'Lateral pressure in membranes', *Biochimica et Biophysica Acta - Reviews on Biomembranes*, 1286(3), pp. 183–223. doi: 10.1016/S0304-4157(96)00009-3.

Martinez, J. C. *et al.* (2013) 'Isothermal Titration Calorimetry: Thermodynamic Analysis of the Binding Thermograms of Molecular Recognition Events by Using Equilibrium Models', in *Applications of Calorimetry in a Wide Context - Differential Scanning Calorimetry, Isothermal Titration Calorimetry and Microcalorimetry*, p. 28.

De Martino, L. *et al.* (2010) 'The antigerminative activity of twenty-seven monoterpenes', *Molecules*, 15(9), pp. 6630–6637. doi: 10.3390/molecules15096630.

Masserini, M. and Ravasi, D. (2001) 'Role of sphingolipids in the biogenesis of membrane domains', *Biochimica et Biophysica Acta - Molecular and Cell Biology of Lipids*, 1532(3), pp. 149–161. doi: 10.1016/S1388-1981(01)00128-7.

Mateen, S. *et al.* (2019) 'Anti-oxidant and anti-inflammatory effects of cinnamaldehyde and eugenol on mononuclear cells of rheumatoid arthritis patients', *European Journal of Pharmacology*. Elsevier B.V., 852(February), pp. 14–24. doi: 10.1016/j.ejphar.2019.02.031.

Matos, J. P. S. C. F. *et al.* (2018) 'Citronellol, a monoterpene alcohol with promising pharmacological activities - A systematic review', *Food and Chemical Toxicology*. Elsevier, 123(November 2018), pp. 459–469. doi: 10.1016/j.fct.2018.11.030.

Melo, M. S. *et al.* (2010) 'Antinociceptive effect of citronellal in mice', *Pharmaceutical Biology*, 48(4), pp. 411–416. doi: 10.3109/13880200903150419.

Melo, M. S. *et al.* (2011) 'Anti-inflammatory and redox-protective activities of citronellal', *Biological Research*, 44(4), pp. 363–368. doi: 10.4067/S0716-97602011000400008.

Minami, A. *et al.* (2009) 'Alterations in detergent-resistant plasma membrane microdomains in Arabidopsis thaliana during cold acclimation', *Plant and Cell Physiology*, 50(2), pp. 341–359. doi: 10.1093/pcp/pcn202.

Mnif, W. *et al.* (2016) 'Essential Oils' Chemical Characterization and Investigation of Some Biological Activities: A Critical Review', *Medicines*, 3(4), p. 25. doi: 10.3390/medicines3040025.

Moe, P. and Blount, P. (2005) 'Assessment of potential stimuli for mechano-dependent gating of MscL: Effects of pressure, tension, and lipid headgroups', *Biochemistry*, 44(36), pp. 12239–12244. doi: 10.1021/bi0509649.

Mongrand, S. *et al.* (2010) 'Membrane rafts in plant cells', *Trends in Plant Science*. Elsevier Current Trends, 15(12), pp. 656–663. doi: 10.1016/J.TPLANTS.2010.09.003.

Mortimer, A. M. (1997) 'Phenological adaptation in weeds - An evolutionary response to the use of herbicides?', *Pesticide Science*, 51(3), pp. 299–304. doi: 10.1002/(SICI)1096-9063(199711)51:3<299::AID-PS653>3.0.CO;2-I.

Namer, B. *et al.* (2005) 'TRPA1 and TRPM8 activation in humans: Effects of cinnamaldehyde and menthol', *NeuroReport*, 16(9), pp. 955–959. doi: 10.1097/00001756-200506210-00015.

Nazzaro, F. *et al.* (2017) 'Essential oils and antifungal activity', *Pharmaceuticals*, 10(4), pp. 1–20. doi: 10.3390/ph10040086.

Nosé, S. (1984) 'A molecular dynamics method for simulations in the canonical ensemble', *Molecular Physics*, 52(2), pp. 255–268. doi: 10.1080/00268970110089108.

Nowotarska, S. W. *et al.* (2014) 'Effect of structure on the interactions between five natural

antimicrobial compounds and phospholipids of bacterial cell membrane on model monolayers', *Molecules*, 19(6), pp. 7497–7515. doi: 10.3390/molecules19067497.

De Oliveira Pereira, F. *et al.* (2015) 'Antifungal activity of geraniol and citronellol, two monoterpenes alcohols, against Trichophyton rubrum involves inhibition of ergosterol biosynthesis', *Pharmaceutical Biology*, 53(2), pp. 228–234. doi: 10.3109/13880209.2014.913299.

Oostenbrink, C. *et al.* (2004) 'A biomolecular force field based on the free enthalpy of hydration and solvation: The GROMOS force-field parameter sets 53A5 and 53A6', *Journal of Computational Chemistry*, 25(13), pp. 1656–1676. doi: 10.1002/jcc.20090.

Osteen, C. D. and Fernandez-Cornejo, J. (2016) 'Herbicide Use Trends : A Backgrounder', 31, pp. 1–7.

Owen, M. D. K. (2016) 'Diverse Approaches to Herbicide-Resistant Weed Management', *Weed Science*, 64(sp1), pp. 570–584. doi: 10.1614/ws-d-15-00117.1.

Parrinello, M. and Rahman, A. (1981) 'Polymorphic transitions in single crystals: A new molecular dynamics method', *Journal of Applied Physics*, 52(12), pp. 7182–7190. doi: 10.1063/1.328693.

Pavela, R. (2015) 'Essential oils for the development of eco-friendly mosquito larvicides: A review', *Industrial Crops and Products*. Elsevier, 76, pp. 174–187. doi: 10.1016/J.INDCROP.2015.06.050.

Poonpaiboonpipat, T. *et al.* (2013) 'Phytotoxic effects of essential oil from Cymbopogon citratus and its physiological mechanisms on barnyardgrass (Echinochloa crus-galli)', *Industrial Crops and Products*. Elsevier, 41, pp. 403–407. doi: 10.1016/J.INDCROP.2012.04.057.

Radhakrishnan, R., Alqarawi, A. A. and Abd_Allah, E. F. (2018) 'Bioherbicides: Current knowledge on weed control mechanism', *Ecotoxicology and Environmental Safety*. Elsevier Inc., 158(November 2017), pp. 131–138. doi: 10.1016/j.ecoenv.2018.04.018.

Rajkumar, V. *et al.* (2019) 'Toxicity, antifeedant and biochemical efficacy of Mentha piperita L. essential oil and their major constituents against stored grain pest', *Pesticide Biochemistry and Physiology*. Academic Press, 156, pp. 138–144. doi: 10.1016/J.PESTBP.2019.02.016.

Razafindralambo, H. *et al.* (2009) 'Thermodynamic studies of the binding interactions of surfactin analogues to lipid vesicles: Application of isothermal titration calorimetry', *Journal of Thermal Analysis and Calorimetry*, 95(3), pp. 817–821. doi: 10.1007/s10973-008-9403-6.

Reichling, J. *et al.* (2009) 'Essential oils of aromatic plants with antibacterial, antifungal, antiviral, and cytotoxic properties - An overview', *Forschende Komplementarmedizin*, 16(2), pp. 79–90. doi: 10.1159/000207196.

Ribeiro, A. V. *et al.* (2018) 'Selection of an essential oil from Corymbia and Eucalyptus plants against Ascia monuste and its selectivity to two non-target organisms', *Crop Protection*. Elsevier, 110, pp. 207–213. doi: 10.1016/J.CROPRO.2017.08.014.

Searchinger, T. *et al.* (2013) 'Creating a Sustainable Food Future: Interim Findings', *World Resources Institute, WRI*, p. 154. Available at: http://www.wri.org/publication/creating-sustainable-food-future-interim-findings.

Semeniuc, C. A., Pop, C. R. and Rotar, A. M. (2017) 'Antibacterial activity and interactions of plant essential oil combinations against Gram-positive and Gram-negative bacteria', *Journal of Food and Drug Analysis*. Elsevier, 25(2), pp. 403–408. doi: 10.1016/J.JFDA.2016.06.002.

Sharma, Y. *et al.* (2019) ' β-citronellol alters cell surface properties of Candida albicans to influence pathogenicity related traits ', *Medical Mycology*, pp. 1–14. doi: 10.1093/mmy/myz009.

Shen, S. *et al.* (2015) 'Effects of cinnamaldehyde on Escherichia coli and Staphylococcus aureus membrane', *Food Control*. Elsevier Ltd, 47, pp. 196–202. doi: 10.1016/j.foodcont.2014.07.003.

Shreaz, S. *et al.* (2010) 'Anticandidal activity of cinnamaldehyde, its ligand and Ni(II) complex: Effect of increase in ring and side chain', *Microbial Pathogenesis*. Elsevier Ltd, 49(3), pp. 75–82. doi: 10.1016/j.micpath.2010.03.013.

Shreaz, S. *et al.* (2016) 'Cinnamaldehyde and its derivatives, a novel class of antifungal agents', *Fitoterapia*. Elsevier B.V., 112, pp. 116–131. doi: 10.1016/j.fitote.2016.05.016.

Singh, H. P. *et al.* (2002) 'Comparative phytotoxicity of four monoterpenes against Cassia occidentalis', *Annals of Applied Biology*, 141(2), pp. 111–116. doi: 10.1111/j.1744-7348.2002.tb00202.x.

Singh, H. P. *et al.* (2004) 'Weed suppressing ability of some monoterpenes', *Zeitschrift Fur Pflanzenkrankheiten Und Pflanzenschutz-Journal of Plant Diseases and Protection*, (19), pp. 821–828.

Singh, H. P. *et al.* (2006) 'Phytotoxicity of the volatile monoterpene citronellal against some weeds', *Zeitschrift fur Naturforschung - Section C Journal of Biosciences*, 61(5–6), pp. 334–340.

Singh, H. P. *et al.* (2009) 'Essential oil of Artemisia scoparia inhibits plant growth by generating reactive oxygen species and causing oxidative damage', *Journal of Chemical Ecology*, 35(2), pp. 154–162. doi: 10.1007/s10886-009-9595-7.

Singh, S., Fatima, Z. and Hameed, S. (2016) 'Citronellal-induced disruption of membrane homeostasis in Candida albicans and attenuation of its virulence attributes', *Revista da Sociedade Brasileira de Medicina Tropical*, 49(4), pp. 465–472. doi: 10.1590/0037-8682-0190-2016.

Stambulchik, E. (2015) 'GRaphing, Advanced Computation and Exploration of data'.

Sterrett, F. S. (1962) 'The nature of essential oils. II. Chemical constituents, analysis', *Journal of Chemical Education*, 39(5), pp. 246–251. doi: 10.1021/ed039p246.

Subash Babu, P., Prabuseenivasan, S. and Ignacimuthu, S. (2007) 'Cinnamaldehyde-A potential antidiabetic agent', *Phytomedicine*, 14(1), pp. 15–22. doi: 10.1016/j.phymed.2006.11.005.

Tabari, M. A. *et al.* (2017) 'Toxicity of β-citronellol, geraniol and linalool from Pelargonium roseum essential oil against the West Nile and filariasis vector Culex pipiens (Diptera: Culicidae)', *Research in Veterinary Science*, 114, pp. 36–40. doi: 10.1016/j.rvsc.2017.03.001.

Tao, N., Jia, L. and Zhou, H. (2014) 'Anti-fungal activity of Citrus reticulata Blanco essential oil against Penicillium italicum and Penicillium digitatum', *Food Chemistry*. Elsevier Ltd, 153(November 2011), pp. 265–271. doi: 10.1016/j.foodchem.2013.12.070.

Tidgewell, K., Clark, B. R. and Gerwick, W. H. (2010) 'The Natural Products Chemistry of Cyanobacteria', *Comprehensive Natural Products II*. Elsevier, pp. 141–188. doi: 10.1016/B978-008045382-8.00041-1.

Tieleman, D. P. (2018) 'Biocomputing Group University of Calgary'. Available at: http://wcm.ucalgary.ca/tieleman/downloads.

Tsagareli, M. G. *et al.* (2010) 'Behavioral evidence of thermal hyperalgesia and mechanical allodynia induced by intradermal cinnamaldehyde in rats', *Neuroscience Letters*. Elsevier Ireland Ltd, 473(3), pp. 233–236. doi: 10.1016/j.neulet.2010.02.056.

Tworkoski, T. (2006) 'Herbicide effects of essential oils', *Weed Science*, 50(4), pp. 425–431. doi: 10.1614/0043-1745(2002)050[0425:heoeo]2.0.co;2.

Uemura, M. and Joseph, R. A. (1995) 'Cold Acclimation of Arabidopsis thaliana: Effect on Plasma Membrane Lipid Composition and Freeze-lnduced Lesions', *Plant Physiology*, 1(109), pp. 15–30.

Vermeer, L. S. *et al.* (2007) 'Acyl chain order parameter profiles in phospholipid bilayers: Computation from molecular dynamics simulations and comparison with 2H NMR experiments',

European Biophysics Journal, 36(8), pp. 919–931. doi: 10.1007/s00249-007-0192-9.

Wayne, R. (2019) 'Plasma Membrane', *Comprehensive Membrane Science and Engineering*. doi: 10.1016/B978-0-08-093250-7.00045-1.

Wewer, V. *et al.* (2011) 'Quantification of sterol lipids in plants by quadrupole time-of-flight mass spectrometry', *Journal of Lipid Research*, 52(5), pp. 1039–1054. doi: 10.1194/jlr.d013987.

Zhang, W. (2018) 'Global pesticide use: Profile, trend, cost / benefit and more', *Proceedings of the International Academy of Ecology and Environmental Sciences*, 8(1), pp. 1–27. Available at: http://www.iaees.org/publications/journals/np/articles/cn/.

Zore, G. B. *et al.* (2011) 'Terpenoids inhibit Candida albicans growth by affecting membrane integrity and arrest of cell cycle', *European Journal of Integrative Medicine*. Elsevier GmbH., 18(13), pp. 1181–1190. doi: 10.1016/j.phymed.2011.03.008.

ANNEXES

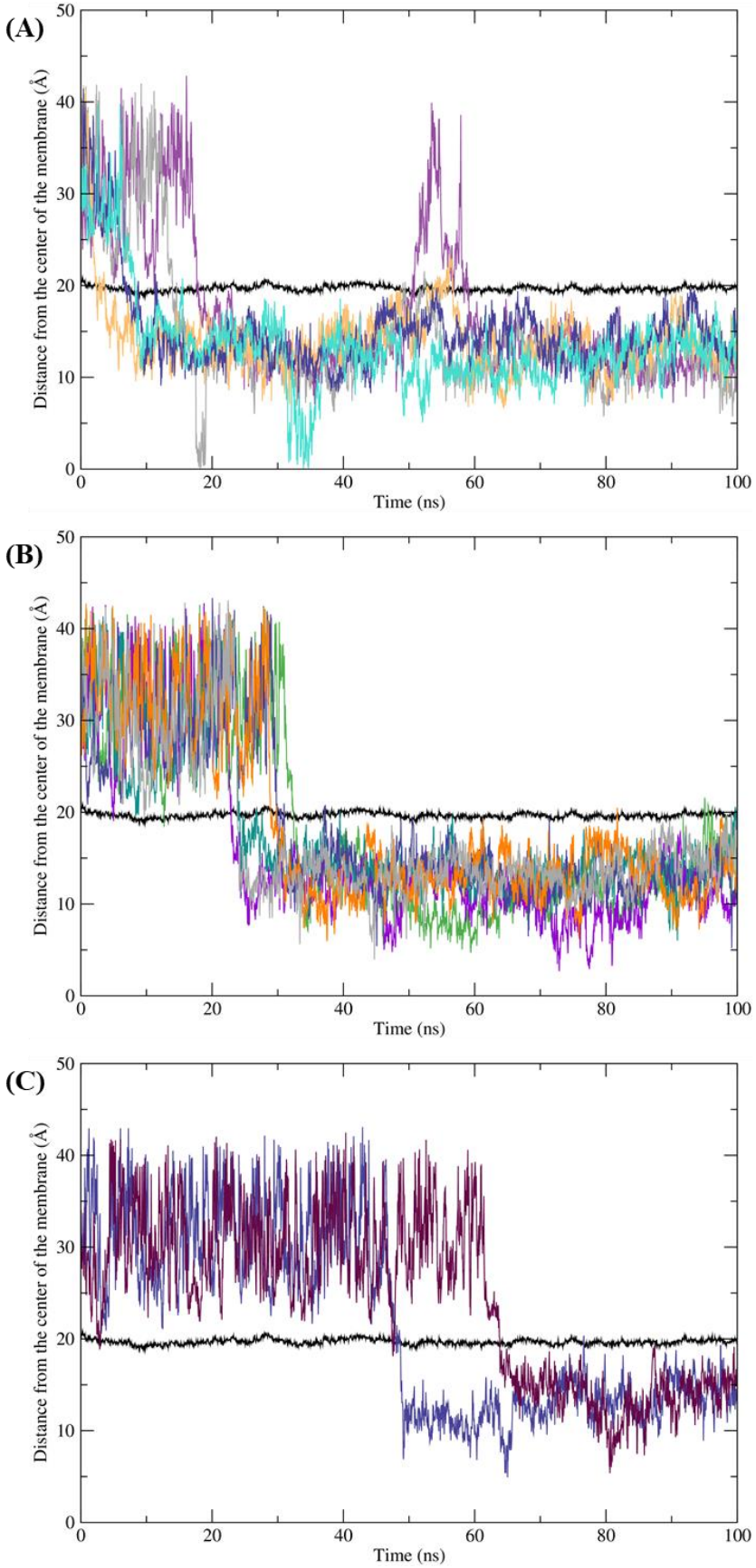

Figure S1: Evolution of the distance in Angstrom between mass centre of the membrane and CIN molecules penetrating the membrane (A) before 20ns, (B) between 20 and 40ns and (C) after 40ns. Black: mean distance between the mass centre of phosphate atoms of the PLPC molecules and the membrane, colours: distance between the mass centre of herbicidal molecules and the mass centre of the membrane.

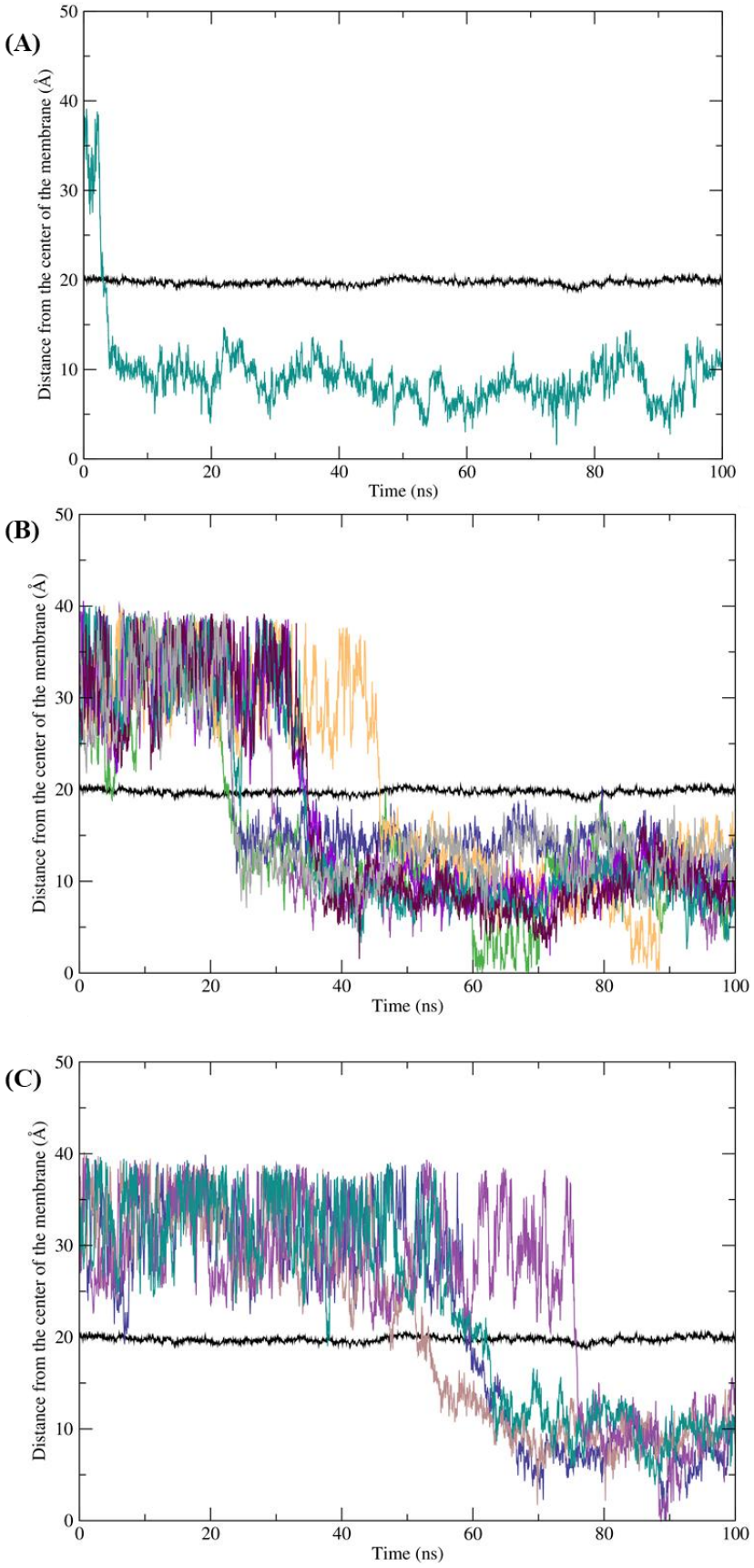

Figure S2: Evolution of the distance in Angstrom between mass centre of the membrane and CitA molecules penetrating the membrane (A) before 20ns, (B) between 20 and 50ns and (C) after 50ns. Black: mean distance between the mass centre of phosphate atoms of the PLPC molecules and the membrane, colours: distance between the mass centre of herbicidal molecules and the mass centre of the membrane.

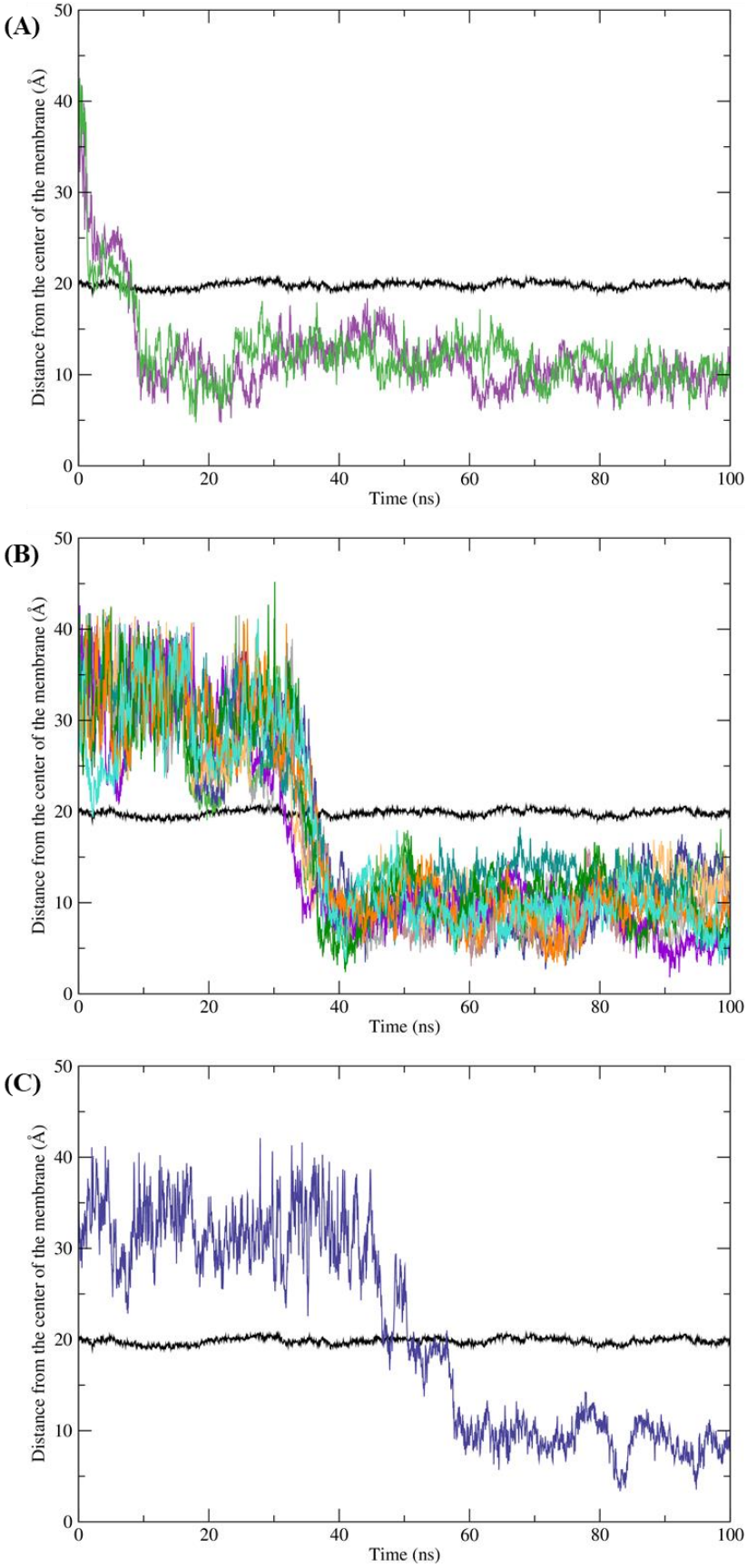

Figure S3: Evolution of the distance in Angstrom between mass centre of the membrane and CitO molecules penetrating the membrane (A) before 20ns, (B) between 20 and 50ns and (C) after 50ns. Black: mean distance between the mass centre of phosphate atoms of the PLPC molecules and the membrane, colours: distance between the mass centre of herbicidal molecules and the mass centre of the membrane.